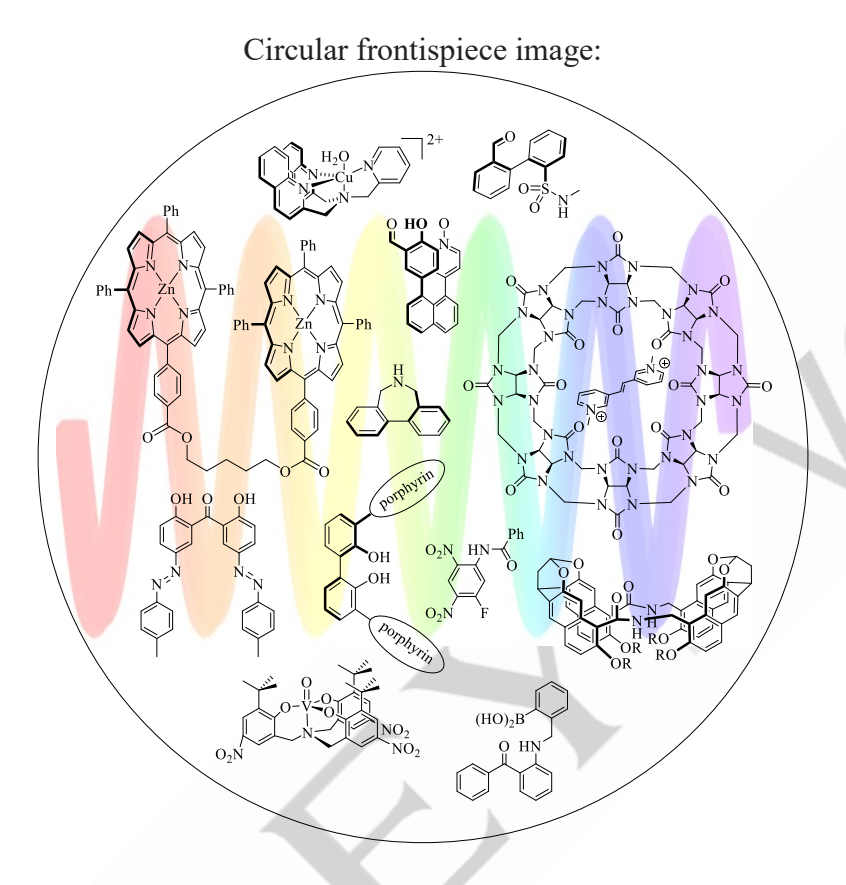
Circular Dichroism Sensing: Strategies and Applications

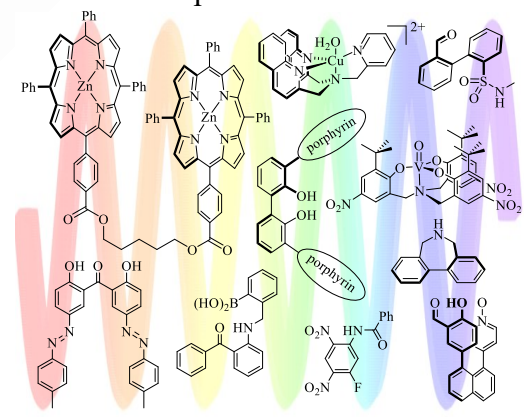
Jeffrey S. S. K. Formen, 1 James R. Howard, 2 Eric V. Anslyn, *2 Christian Wolf*1



Keywords: chirality; absolute configuration; enantiomeric excess; high-throughput screening; optical sensors

TOC:

Chiroptical sensing of the absolute configuration, enantiomeric ratio and concentration of organic compounds has developed into a mature field with practical applications, including high-throughput asymmetric reaction screening and chromatography-free analysis of multicompound mixtures. This review covers fundamental milestones and highlights recent advances with machine learning assistance, chemometric data processing and other developments.



[1] J. S. S. K. Formen, C. Wolf Chemistry Department Georgetown University Washington DC, USA E-mail: cw27@georgetown.edu

J. R. Howard, E. V. Anslyn Chemistry Department University of Texas at Austin

Austin TX, USA

Email: anslyn@austin.utexas.edu

The analysis of the absolute configuration, enantiomeric composition, and concentration of chiral compounds are frequently encountered tasks across the chemical and health sciences. Chiroptical sensing methods can streamline this work and allow high-throughput screening with remarkable reduction of operational time and cost. During the last few years, significant methodological advances with innovative chirality sensing systems, the use of computer-generated calibration curves, machine learning assistance, and chemometric data processing, to name a few, have emerged and are now matched with commercially available multi-well plate CD readers. These developments have reframed the chirality sensing space and provide new opportunities that are of interest to a large group of chemists. This review will discuss chirality sensing strategies and applications with representative small-molecule CD sensors. Emphasis will be given to important milestones and recent advances that accelerate chiral compound analysis by outperforming traditional methods, conquer new directions, and pioneering efforts that lie at the forefront of chiroptical high-throughput screening developments. The goal is to provide the reader with a thorough understanding of the current state and a perspective of future directions of this rapidly emerging field.

1. Introduction

The ubiquity, fundamental significance, and far-reaching implications of small-molecule chirality in the chemical and life sciences are staggering and continue to inspire technological innovation and chemical developments. Academic and industrial laboratories frequently encounter the need to determine the absolute configuration, concentration and enantiomeric composition of chiral compounds that occur in biological media, are generated during asymmetric synthesis discoveries, or play a crucial role in R&D and manufacturing. Typically, these samples are complex mixtures and pose several challenges. Traditional methods that have been predominantly used require purification of the chiral compounds of interest prior to the quantitative analysis, which makes this task tedious, labor-intensive, timeconsuming and often produces a considerable amount of waste. In addition, time pressure and expectations of processing hundreds of samples in parallel to improve laboratory productivity and turnaround ought to be matched. In principle, this is possible with generally available high-throughput experimentation (HTE) equipment, but the full capacity of state-of-the-art screening technology cannot be reached when inherently serial analytical techniques are employed. This is the case with chiral chromatography or electrophoresis methods which are restricted to time-inefficient one-sample-at-a-time protocols although it is noteworthy that high-speed separations have been reported.1 Given the well-known shortcomings of GC, SFC and HPLC, methods based on mass spectrometry, 2 UV3 and fluorescence4 spectroscopy, gas-phase rotational resonance spectroscopy, 5 IR

(ECD),7 thermography,6 electronic circular dichroism CD,8 fluorescence-detected NMR spectroscopy,9 biochemical procedures¹⁰ have emerged. To this end, perhaps the most persuasive methodical advances and real-world applications have been achieved with chiroptical sensing assays that are amenable to HTE workflows and capable of simultaneous concentration and enantiomeric excess (ee) determination of increasingly challenging samples without compound purification.11

Jeffrey S. S. K. Formen received his B.A. in Biochemistry from Middlebury College in 2019, where he worked in the Repka laboratory. Currently he is pursuing his Ph.D. at Georgetown University under the guidance of Professor Christian Wolf. His research focuses on synthetic methodology development, chiral recognition, quantitative ee analysis, and optical sensing of chiral compounds.



James Howard earned his Ph.D. in chemistry from the University of Texas at Austin under the supervision of Professor Eric V. Anslyn. His research focused on the application of machine learning protocols to chiroptical assays. He is currently a postdoctoral researcher at the University of Utah, where he develops new machine learning techniques for enhanced



Eric V. Anslyn received his PhD under the direction of Robert Grubbs at the Caltech in 1987. Afterwards, he was an NSF post-doctoral fellow at Columbia University, working with Ronald Breslow. From there he started as an assistant professor of chemistry at the University of Texas at Austin in 1989. At UT Austin he rose through the ranks to currently hold the Welch Regents Chair of Chemistry, and is a University Distinguished Teaching Professor, as well as an HHMI Professor.



Christian Wolf obtained his Ph.D. under the supervision of Wilfried König at the University of Hamburg, Germany, in 1995. After postdoctoral studies as Feodor Lynen Fellow with William Pirkle at the University of Illinois, he worked several years in R&D at SmithKline Beecham Pharmaceuticals. In 2000, he started as Assistant Professor at Georgetown University in Washington, DC, where he was appointed Associate Professor with tenure

in 2006, Full Professor in 2011, and Director of Medicinal Chemistry in 2017.





Figure 1. Structures of selected CD probes.

The use of CD spectroscopy for chiral compound analysis seems a logical choice given its intrinsic ability to differentiate between enantiomers. However, many chiral compounds do not display distinct circular dichroism spectra and require the utilization of chromophoric reporters that are designed to bind the target molecule and to generate chiroptical signals suitable for stereochemical identification or quantification of the enantiomeric composition. The practicality of this approach for absolute configuration determination has been verified numerous times, especially by Nakanishi, Berova, Canary, Gawronski, Rosini and Borhan who have introduced an impressive suite of probes, includina zinc-porphyrin tweezers, that allow interpretation of the induced Cotton effects obtained upon covalent substrate binding or metal coordination, Figure 1.12-33 Because the sign of the generated CD curves is causally linked to the chirality of the analyte it reveals its absolute configuration. Quantitative ee analysis is also possible and has been demonstrated numerous times with a very broad range of chiral compounds by Anslyn, 34-43 Nau and Biedermann, 44,45 Jiang, 46-49 Zonta, 50-55 Wolf 56-65 and through collaborative efforts from Chin, Hong and Kim⁶⁶⁻⁶⁸ as well as Baik, Yoon and Kim.⁶⁹ These and several other laboratories⁷⁰⁻⁷⁶ have developed assays that make use of the intensity of the induced CD amplitudes which is readily correlated to the ee of the analyte with the help of a calibration curve. The underlying binding motifs applied in these tasks span the whole repertoire of organic, coordination and supramolecular chemistries, and range from reversible equilibria controlled by weak forces, or reversible covalent interactions, to irreversible bond formation. A large selection of probes, of which only a few are depicted in Figure 1, is nowadays available and ready for adoption by any laboratory interested in stereochemical analysis. Assays that are based on click chemistry, metal coordination, formation of a Schiff base or dynamic covalent assemblies, and host-guest interactions have become most popular and shown to

be well suited for a variety of applications. Examples include accelerated asymmetric reaction development, quantification of chiral biomarkers such as free D-amino acids, and analysis of mixtures containing enantiomers and diastereomers or chemically related chiral compounds, which are all challenging tasks that can now be achieved in real high-throughput fashion by skipping tedious chromatography steps.

This Review aims to highlight chirality sensing strategies and applications with representative small-molecule CD sensor systems. Particular emphasis is given to important milestones and recent advances that streamline chiral compound analysis by outperforming traditional methods, conquer new opportunities, and according to the authors' opinion lie at the forefront of chiroptical high-throughput screening developments. The goal is to provide the reader with a thorough understanding of the current state and a perspective of future directions of this rapidly emerging field.

2. Absolute Configuration Analysis

Many CD methods for the determination of the absolute configuration of chiral compounds, of which some are empirical and limited to cases where a reference or literature reports are available for comparison, have been developed. Intramolecular interactions between two or more non-conjugated chromophores showing electric dipole allowed electronic transitions give rise to exciton-coupled circular dichroism (ECCD), which can be used for reliable assignments of new compounds and natural products. This non-empirical approach is a powerful tool for chemists, but its use is not trivial and typically requires computational assistance. A thorough conformational analysis, knowledge of the chromophore electric transition dipole moments, and careful

couplet inspection (for example to rule out interferences from other CD effects), are essential for reliable interpretation.⁷⁷⁻⁷⁹

2.1. Covalently Attached Probes

A variety of derivatization protocols that allow absolute configuration determination of amines, alcohols, diols, amino alcohols, carboxylic acids, amino acids and other important compound classes, for example with naphtol, 80,81 phthalimide 82-84 and dinaphthyl ketal reagents, 23 are available. Stereodynamic biaryl probes have become a privileged design motif and been thoroughly investigated. 85-87 The covalent attachment of chiral carboxylic acids 1 to the biphenyl-derived azepine probe 2 yields amides 3 which after purification are suitable for stereochemical analysis. 19,88 The point chirality of the bound substrate is imprinted onto the stereodynamic biphenyl moiety through the planar amide bond and the conformationally restricted seven-membered ring, Figure 2. Rosini showed that this gives rise to characteristic CD signals which, in turn, can be rationally correlated to the absolute configuration of the carboxylic acid.

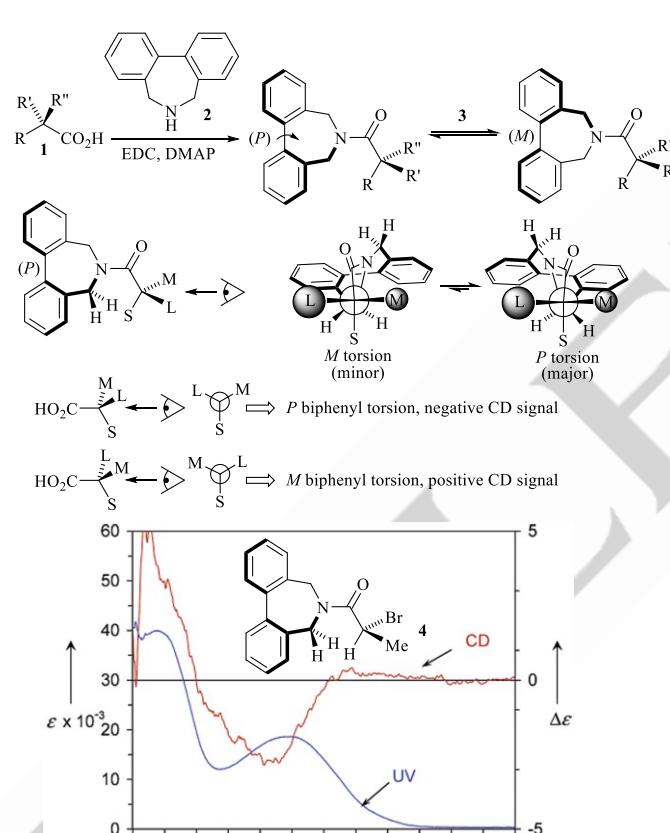


Figure 2. Attachment of the azepine probe **2** to carboxylic acids **1** and stereochemical assignment based on minimized steric interactions (top). UV and CD spectra of the azepine derivative of (*S*)-2-bromopropionic acid **4** (bottom). Note that the *A* values are 0.48-0.67 kcal/mol for Br and 1.74 kcal/mol for Me. EDC (1-ethyl-3-(3-dimethylaminopropyl)carbodiimide), DMAP (4-dimethlyaminopyridine). Reprinted with permission from ref. [19]. Copyright 2006 American Chemical Society.

260

280

240

300

320 nm

220

200

In the most stable conformation, the smallest group S at the chiral center resides in the amide bond plane and between the adjacent azepine protons. The biphenyl, which serves as the CD reporter unit, adopts a twisted structure to minimize steric repulsion with

the largest residue L. When the substituents L, M and S share a clockwise orientation this process results in P torsion and is associated with a negative CD amplitude at approximately 240 nm. Incorporation of the carboxylic acid enantiomer reverses the bias to the M-biphenyl conformer and consequently generates the opposite CD response. It is critical that the size of the three substituents L, M and S is carefully compared based on steric A values, which are readily available from the literature, to avoid incorrect interpretation. Finally, a different model accounting for π -stacking interactions is required when α -aryl carboxylic acids are applied in the azepine derivatization assay.

The same group showed that diols $\bf 5$ undergo smooth ketal formation with $\bf 6$ toward spiro compounds $\bf 7$ exhibiting a bridged biphenyl unit that becomes CD-active, Figure $\bf 3.^{14.89}$ These compounds exist as a rapidly equilibrating mixture of diastereomers in which the diol chirality dictates the biaryl twist and consequently the induced CD signals. Generally, substrates with R-configuration shift the equilibrium toward the M-isomer while S-diols favor population of the P-biphenyl conformer. The predictability of central-to-axial chirality induction and of the corresponding CD sign at 250 nm thus enables absolute configuration analysis with a single measurement.

Figure 3. Rosini's diol sensing with ketal 6.

The trityl group is not only a popular protecting group for alcohols and amines, it exhibits so-called propeller chirality and can therefore be used for absolute configuration determination when attached to chiral substrates, Figure 4.90.91 Gawronski studied a variety of trityl ethers such as 8 and found that the *MPM*-propeller giving a negative CD couplet is typically favored when the alcohol moiety has S configuration, while a *PMP*-conformation with a positive Cotton effect is adapted by trityl ethers of R alcohols. Stereochemical assignments based on chiroptical measurements with trityl amines is possible, but the rationalization of the CD inductions is more complicated because of contributions from N-inversion processes.

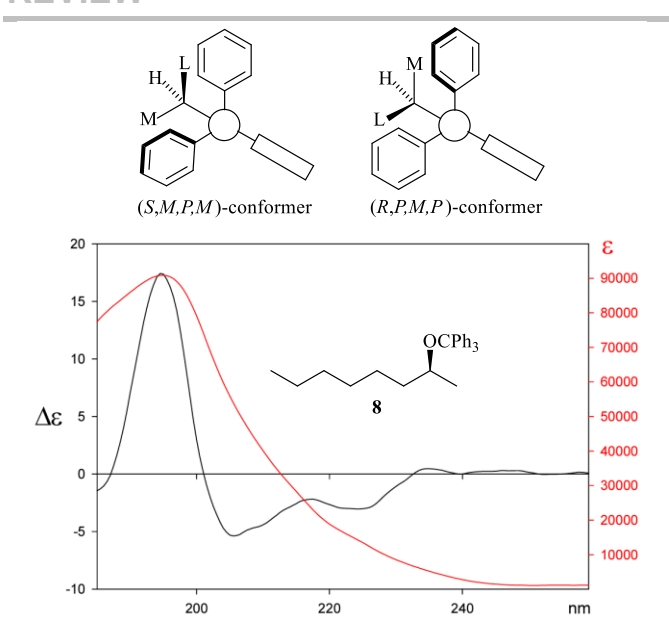


Figure 4. Schematic showing the residual *MPM*- and *PMP*-conformations of trityl ethers derived from secondary alcohols and chiroptical analysis of (*S*)-2-octyl trityl ether. The Newman projection is along the O-trityl bond showing the oxygen atom on top. Reprinted with permission from the SI in ref. [90]. Copyright 2009 John Wiley & Sons.

2.2. Metal Coordination Complexes

The Canary group was among the first to recognize the usefulness of metal coordination complexes for chiroptical analysis. They found that the reaction of an amino acid with two equivalents of 2-bromomethylquinoline affords a polydentate ligand generating a distinctively twisted coordination sphere around copper(II) or other metal centers. The point stereocenter controls the propeller-like arrangement of the proximate heteroaryl rings and ultimately the resultant ECCD effects. Incorporation of L-amino acids yields a counterclockwise orientation resulting in a negative CD couplet centered at approximately 230 nm. By contrast, D-amino acids favor a clockwise arrangement with a positive Cotton effect. The observed CD spectra can thus be used for determination of the absolute configuration of the amino acid, as shown for the (S)-methionine derived Cu(II) complex 9 in Figure 5. 93-95

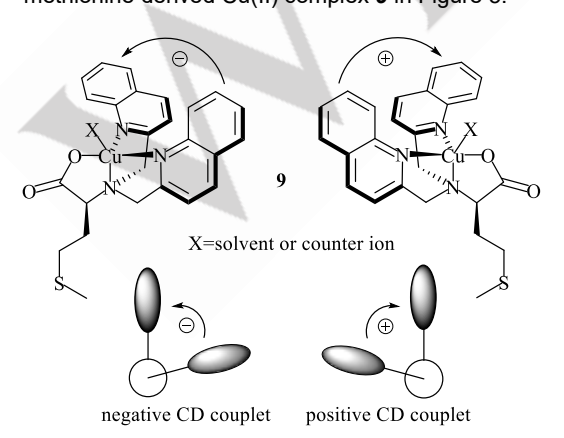


Figure 5. Relation between the quinoline twists in the (S)-and (R)-methionine derived Cu(II) complex 9 and the corresponding ECCD signals.

The same concept has been exploited with copper and zinc complexes of polydentate quinolyl and pyridyl ligands derived from chiral alcohols, amino alcohols or amines. 18,96 This pioneering work was later extended by Anslyn, Di Bari and Canary who designed multicomponent assemblies around a transition metal center for absolute stereochemical assignments and practical ee analysis, *vide infra*.

Metalloporphyrins have been applied in the stereochemical analysis of amino esters,97 carbohydrates,98 carboxylic acids,99 other small molecules 100 and secondary DNA structures. 101 In most cases, relatively weak Cotton effects were produced but the obvious potential of this approach initiated groundbreaking developments with tweezer-like analogs displaying metalloporphyrin rings connected via a covalently attached linker. The presence of two proximate large chromophores, both accessible and able to hold a difunctional chiral substrate, enables ECCD sensing which has proven highly advantageous by Nakanishi and Berova. 25,102 The tweezer 10 shown in Figure 6 accommodates the diamine 11 which coordinates to the two zinc centers and thus biases the relative orientation of the porphyrin rings to minimize steric repulsion in 12.103 The induced conformational twist in the tweezer yields bisignate signals due to coupling of the porphyrin electric transition dipole moments, which can be correlated to the absolute configuration of the analyte with the help of a simple model. The flexibility of the aliphatic linker in 10 is an important design feature as it allows coordination of guest molecules of varying size. The underlying binding motif used here, however, requires analytes having two strongly coordinating amino groups.

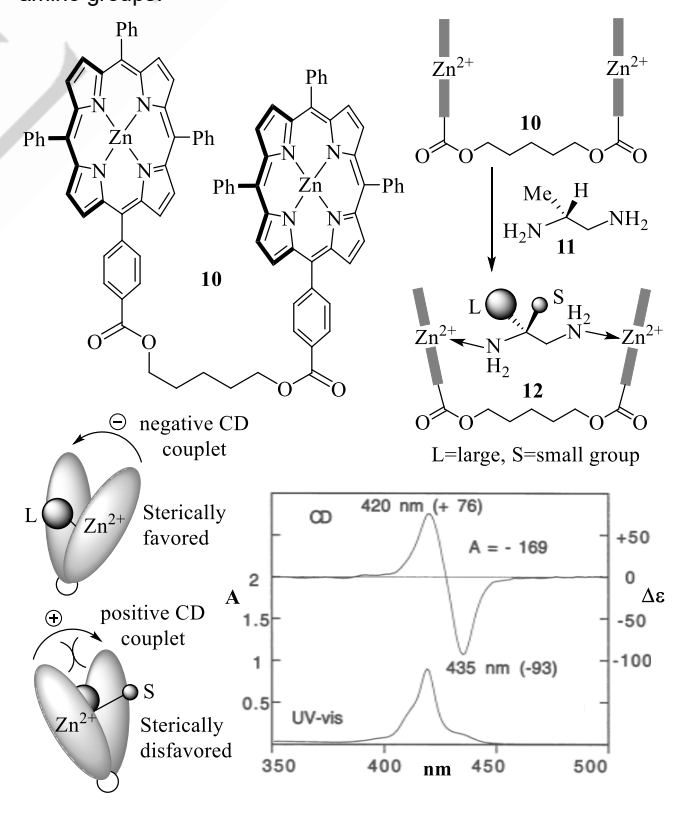


Figure 6. Coordination of a chiral diamine to the zinc(II) centers in tweezer 10 and ECCD and UV spectra obtained with the complex 12 formed with (*R*)-1,2-diaminopropane, 11. Modified with permission from ref [102]. Copyright 2000 John Wiley and Sons.

This limitation has been overcome with the introduction of derivatizing protocols that extend the tweezer method utility by incorporation of a second amino group into substrates that do not fulfill the above criterion. As a result, a large variety of compounds including alcohols, 104,105 amines, 15 amino alcohols, 106 and carboxylic acids 107-110 have become manageable. Tweezers like 10 operate at micromolar concentrations, are applicable to a very wide range of compounds, albeit often only after derivatization with a suitable auxiliary reagent, and generate strong Cotton effects at long wavelengths, which altogether makes them a primary choice for absolute configuration analysis.

Modified bismetalloporphyrins with increasing Lewis acidity or short linkers have been introduced to eliminate the cumbersome need for chemical derivatization prior to the analysis, Figure 7. $^{111-113}$ The success of these modifications has been demonstrated, for example, by Borhan who directly applied the perfluorinated porphyrin tweezer 13 to amino alcohols, epoxy alcohols and diols. 21,114,115 The rigid melamine bridge in 14 effectively shortens the porphyrin separation and reduces the conformational freedom of the two macrocycles which was found to give rise to large Cotton effects upon binding of α -amino esters and amides, secondary alcohols and 1,2-amino alcohols. 116,117

$$C_{6}F_{5}$$

$$C_{6}F_{5}$$

$$Z_{n}$$

$$C_{6}F_{5}$$

$$Z_{n}$$

$$C_{6}F_{5}$$

$$Z_{n}$$

$$C_{6}F_{5}$$

$$Z_{n}$$

$$C_{6}F_{5}$$

$$Z_{n}$$

Figure 7. Examples of perfluorinated and melamine-tethered porphyrin tweezers.

The Borhan group has elevated sensing with porphyrin tweezers to yet another level with their biphenyl-derived MAPOL series, Figure 8.¹¹⁸ These sensors share a stereodynamic bisphenol core that forms a cleft defined by the two porphyrin rings. The two enantiomeric conformers of **15** rapidly interconvert at room temperature via rotation about the pivotal axis and the

mixture remains racemic and therefore chiroptically inactive in the absence of a chiral bias. A chiral amine, 119 sulfoxide, 120 cyanohydrin, 121 or phosphine oxide 122 that diffuses into the cleft may undergo either hydrogen bonding with the phenol groups, coordination to the zinc centers or a combination of both. Importantly, the binding event disturbs the racemic equilibrium and shifts the axial chirality of **15** either toward the P or the M-conformation, resulting in strong ECCD signals at long wavelengths that allow non-empirical assignment of the absolute configuration of the guest molecule with rationally developed and computationally verified mnemonics. An increase in the population of the (P)-bisphenol conformer generally yields a positive ECCD couplet while a negative bisignate CD response is observed when the (M)-bisphenol is favored, for example upon association with (S)-**16**.

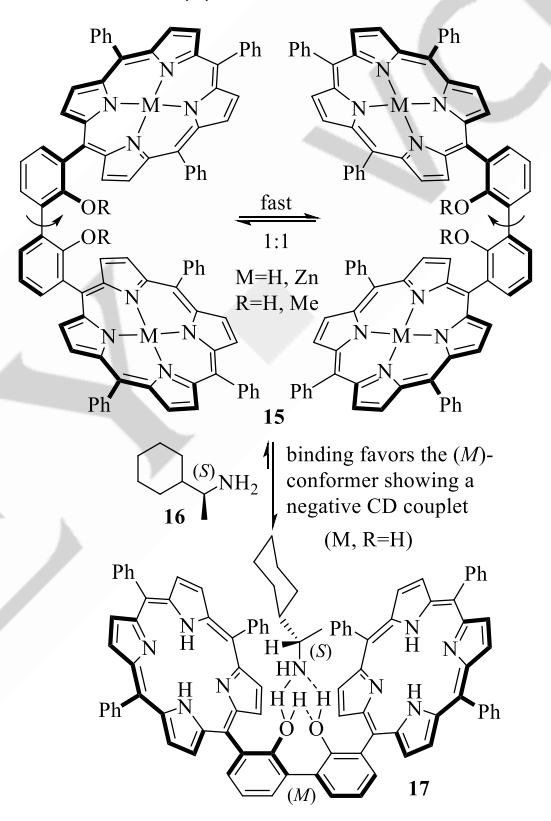
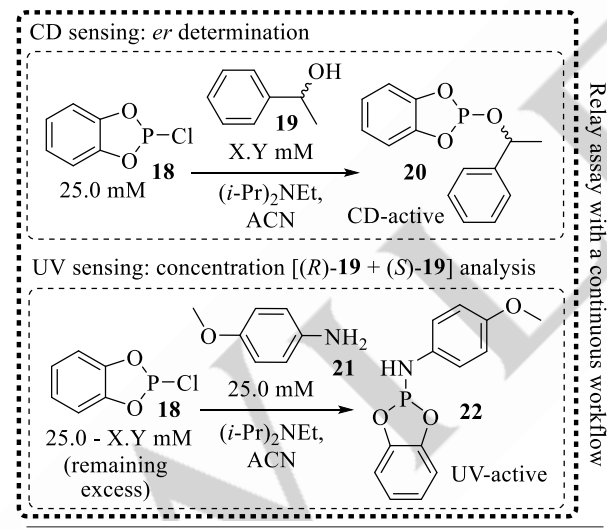


Figure 8. Borhan's stereodynamic MAPOL tweezers and population of the (M)-bisphenol conformation of 17 as a result of hydrogen bonding interactions with an (S)-amine.

3. Sensing of the Enantiomeric Composition of Chiral Compounds

The most successful chiroptical sensing assays rely on broadly applicable chromophoric probes that quickly generate strong CD signals for accurate ee or er (enantiomeric ratio) determination, preferably at wavelengths above 300 nm to avoid potential interferences from optically active impurities. This may be more easily accomplished with analytes carrying an aromatic group that can participate in exciton-coupled CD inductions in cases where there is overlapping absorbance. The general usefulness and scope of a CD assay should therefore be demonstrated with purely aliphatic compounds. In almost all cases, achiral agents that can take full advantage of the enantiomer differentiation

capability of circular dichroism spectroscopy are used, although chiral probes that exhibit modified CD outputs have also been reported. 123 The employment of achiral probes, however, greatly simplifies the analysis by avoiding discrimination effects and systematic errors that may result from the formation of diastereomers. Furthermore, the CD signal induction can coincide with either UV or fluorescence changes that are nonenantioselective when an achiral probe is used as only enantiomeric products are formed. These optical responses therefore allow determination of the total concentration of a chiral compound independent of the enantiomeric composition while the induced CD signals are exploited for absolute configuration and ee analysis. The combination of these optical spectroscopies is very practical and often possible using the same sample only after dilution to adjust for the high sensitivity of UV and fluorescence measurements. Accordingly, probes that generate strong CD spectra simultaneously with quantifiable UV or fluorescence responses are particularly powerful and enable comprehensive concentration and ee analysis at the same time. If the sensor does not fulfill both roles, this can be addressed with a relay assay strategy. 124 Such a relay approach is shown with the chlorophosphite 18, a broadly usable probe for diols, hydroxy acids, amines, and amino alcohols, in Figure 9. First, formation of the phosphite 20 via reaction of 18 with the unknown amount of the chiral alcohol sensing target 19, which could vary substantially but not exceed the concentration of 18, is used for determination of the absolute configuration (AC) and enantiomeric ratio (er) by CD analysis.



	Sample composition			Relay sensing results			
Entry	Conc. (mM)	AC	er	Conc. (mM)	AC	er	
1	6.0	S	83.4:16.6	6.2	S	84.1:15.9	
2	10.0	S	85.0:15.0	9.9	S	82.9:17.1	
3	13.0	R	25.0:75.0	13.8	R	22.3:77.7	
4	16.0	S	71.9:28.1	15.6	S	67.5:32.5	
5	18.0	R	33.3:66.7	18.6	R	34.1:65.9	
6	20.0	S	62.5:37.5	20.5	S	61.8:38.2	
7	24.0	S	97.9:2.1	22.5	S	96.9:3.1	

Figure 9. Chiroptical relay assay using a chlorophosphite that first reacts with a chiral target compound to generate a CD signal for *er* sensing. The excess of the probe is then transformed into a UV-active molecule which allows calculation of the original analyte concentration. AC (absolute configuration).

The remaining excess of unreacted **18** (25.0 - X.Y mM) is then trapped by aniline **21** to give **22** displaying a distinct UV signal that is correlated to the original concentration of **19**. The accuracy of this concept was showcased with samples covering a wide range of concentrations and *er* values.

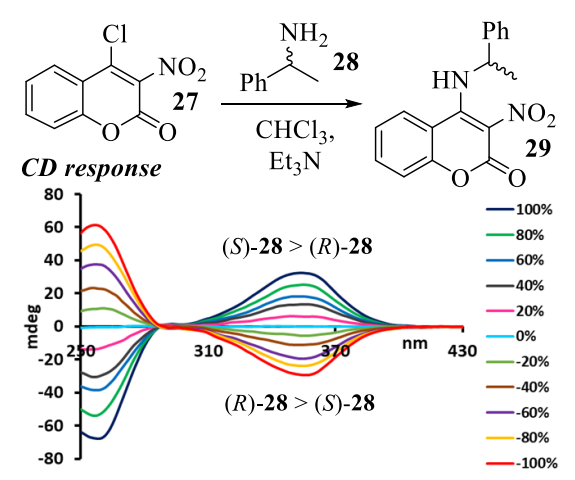
Alternatively, this can be achieved with indicator displacement assay¹²⁵ that release a stoichiometric amount of a UV-active or fluorescent by-product upon binding of the chiral target compound. A biomimetic sensing example that is based on such a strategy is outlined in Figure 10.¹²⁶ The transamination reaction between the pyridoxal-5'-phosphate (PLP) derivative 23, which is CD-silent, and a chiral target 24 exhibiting a primary amino group gives the CD-active Schiff base 25 and results in the simultaneous release of one equivalent of the fluorescent 1-aminonaphthalene, 26, for each molecule of 24. The intrinsic coupling of the generation of these two optically active products in necessarily equimolar amounts is the core concept of the combined CD/fluorescence analysis.

Figure 10. Chirality sensing with a PLP probe generating a stoichiometric amount of a fluorescent indicator for combined CD/fluorescence analysis.

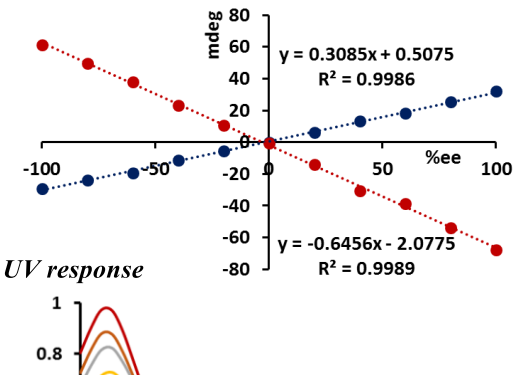
Central to all assays is the molecular recognition event which ideally is sufficiently selective to operate in compound mixtures, chemically well-defined, fast to be compatible with purificationfree high-throughput applications, and capable of generating strong chiroptical signals that can be accurately quantified. The rise of supramolecular chemistry and reversible systems that operate under thermodynamic control has undoubtedly benefited this field and inspired many developments, although rational approaches for example the use of the reciprocity principle 127 or repurposing of well-known chromophoric derivatizing agents previously applied in other fields have also proven successful. A prime example is the introduction of ninhydrin, which is generally used in forensics. 128 Recently, computational guidance and machine learning tools have been introduced to conquer new sensing space, see Chapter 6. The vast majority of chiral compound sensing examples involve either irreversible bond formation with click chemistry features, coordination to metal complexes with stereodynamic ligands, dynamic covalent chemistry, or host-guest complexation while other interactions such as hydrogen bonding have also been utilized. 129,130 In fact, sensor design strategies often integrate more than one of these themes to achieve optimal results.

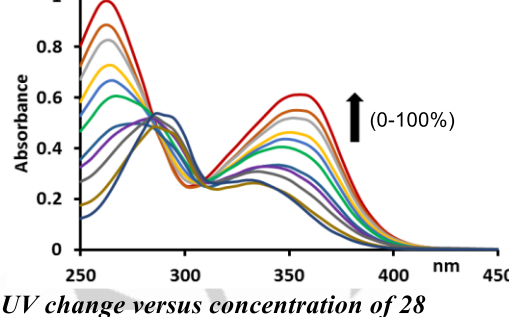
3.1. Click Chemistry

The high speed, robustness, and practicality of click chemistry assays are ideally suited to fully exploit the high-throughput screening (HTS) capacity of chiroptical sensing which has been demonstrated with some of the most compelling examples of chromatography-free asymmetric reaction screening and chiral compound mixture analysis.



Linear correlation between CD maxima and ee





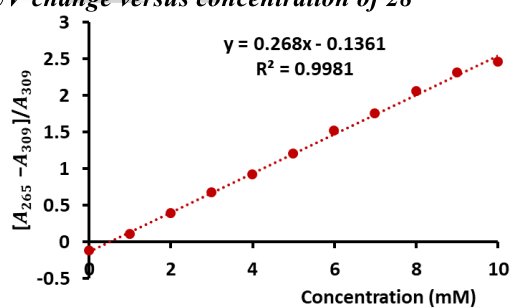


Figure 11. Click chirality sensing with a chlorocoumarin probe. Reproduced from ref. [131] under terms of the CC-BY license.

The general appeal of the Wolf group's chlorocoumarin method originates from the click-like covalent attachment of this privileged chromophore to amines, amino alcohols, amino acids, and alcohols, which is complete in a few minutes and features excellent solvent compatibility, mild conditions and tolerance of air and water unless chiral alcohols are the target compounds, Figure 11.131 This assay has been tested many times with more than 40 compounds and the wide scope, compatibility with HTS equipment, tolerance of chemical impurities and the operational simplicity are outstanding features that have been validated using an automated CD microplate reader. 132 The protocol simply requires mixing of the sample and commercially available 4chloro-3-nitrocoumarin, 27, for 15 minutes and subsequent dilution for chiropical analysis without any work-up. The CD and UV inductions observed with the amine 28 are shown in Figure 11 and serve as a representative example of how chiroptical assays generally work. The CD-silent probe produces a CD response upon formation of 29 which corresponds to the enantiomeric composition of the analyte. Calibration curves of the amplitudes at 257 (red) and 355 (blue) nm are then used to quantify the ee. Linear relationships are obtained with 27 but nonlinear effects are possible with other sensors and are easily analyzed as well. The assay also produces characteristic UV changes that are independent of the sample's ee, and allow determination of the total analyte concentration. Together, the combined UV/CD measurements give the sample concentration, or yield if a reaction is analyzed, and the enantiomeric excess. This can be achieved with minute sample amounts, in fact asymmetric reaction screening with 27 was demonstrated to require only 1 milligram of the crude product mixture.

Chen and Li developed a fast CD/UV sensing assay that allows accurate amino acid analysis even with highly diluted samples, Figure 12.¹³³ The speed of the three-component condensation with commercially available o-phthalaldehyde, **31**, and *p*-toluenethiol, **32**, is very impressive, typically affording the desired isoindole structure **33** under atmospheric conditions in 1-3 minutes. The heteroaryl ring construction coincides with UV and CD inductions showing linear correlations with the amino acid concentration and *ee*, respectively.

	Samp	le comp	osition	Sensing results			
Entry	AC	Conc. (µM)	ee	AC	Conc. (µM)	ee	
1	L-Ala	40.0	60.0	L-Ala	39.2	61.2	
2	D-Ala	10.0	100.0	D-Ala	9.5	99.6	
3	L-Trp	21.0	65.0	L-Trp	22.2	67.2	
4	D-Trp	38.0	79.0	D-Trp	35.8	77.5	

Figure 12. Chiroptical sensing of amino acids at μM concentrations via a three-component click condensation reaction toward isoindoles. AC (absolute configuration).

A large excess of the labeling agents is required to process micromolar sample concentrations, and this assay is not suited for some amino acids including proline and cysteine, which either cannot undergo imine condensation or form multiple products. Nevertheless, most standard amino acids are acceptable targets, and the scope includes unnatural amino acids and dipeptides as well.

Another noteworthy example of click chirality sensing is based on the broadly applicable 2-nitrophenylisocyante probe, 34, which reacts smoothly with a wide range of compounds, including amines, amino alcohols, amino acids, alcohols, and diols.⁶⁴ The click reaction between 34 and compounds carrying a primary or secondary amino group quantitatively yields the corresponding ureas 35 in just 15 minutes, Figure 13. The ureas have strong CD signals at approximately 350 nm and it was shown that simultaneous in situ UV/CD analysis allows for accurate determination of both concentration and ee, eliminating the need for chromatographic separation or any work-up. Importantly, the isocyanate probe is also applicable to the sensing of alcohols, which are challenging targets due to their poor nucleophilicity. In the presence of catalytic amounts of 4-dimethylaminopyridine, DMAP, the reaction with the alcohol substrate forming the corresponding carbamates 36 is complete within 1.5 hours. In analogy to the ureas, the carbamate products provide intense, red-shifted CD signals, that can be used for quantitative analysis, which is exemplarily shown for 37 obtained from 34 and 1-(2naphthyl)ethanol, 38. The wide solvent compatibility of sensing with 34 is another advantageous feature and addresses problems with insufficient solubility of very polar analytes, which often complicates chiral HPLC analysis.

Irreversible substrate binding

$$\begin{array}{c|c}
 & H_2N \\
R & R' \\
\hline
 & R' \\
\hline
 & NCO \\
\hline
 & ST \\
\hline
 & NCO \\
\hline
 & ST \\
\hline
 & NCO \\
\hline
 & ST \\
\hline
 & NO_2 \\
\hline
 & NO_2 \\
\hline
 & NO_2 \\
\hline
 & R' \\
\hline
 & NO_2 \\
\hline
 & R' \\
\hline
 & NO_2 \\
\hline
 & R' \\
\hline
 & R' \\
\hline
 & R' \\
\hline
 & NO_2 \\
\hline
 & R' \\
\hline
 & R' \\
\hline
 & NO_2 \\
\hline
 & R' \\
\hline
 & R' \\
\hline
 & NO_2 \\
\hline
 & R' \\
\hline
 & R' \\
\hline
 & R' \\
\hline
 & NO_3 \\
\hline
 & R' \\
\hline
 & R' \\
\hline
 & NO_3 \\
\hline
 & NO$$

CD & UV response of 34 to samples of 38 at varying

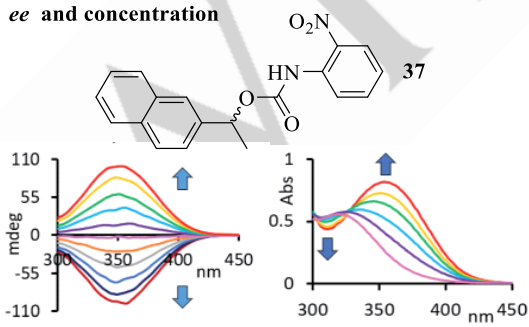


Figure 13. Click chemistry sensing with the arylisocyanate probe **34**. Modified with permission from ref. [64]. Copyright 2021 RSC Publishing.

3.2. Metal Coordination

Many groups have designed stereodynamic metal coordination complexes for chirality sensing. 93,94,106,107,134,135 While this has typically entailed careful ligand development to yield optimal CD induction results, 136,137 ligand-free sensing with cobalt, copper, iron, palladium or other metal salts has also been demonstrated. 138,139 Canary and Anslyn introduced one of the first host-guest systems for chirality sensing with metal coordination complexes, Figure 14.140,141 Their sensing strategy utilized an achiral Cu(II) complex 39 that is CD-silent, easily synthesized, and bears an open coordination site to accommodate a chiral carboxylate guest. Upon binding of a chiral carboxylate, the equilibrium between M- and P-helical stereoisomers is perturbed according to the guest configuration. As a result, substantial Cotton effects are observed at 227 nm and 233 nm around the λ_{max} of the isotropic UV spectrum, which is indicative of ECCD. As with previous examples, the enantiopurity of the carboxylate guest is correlated to the magnitude of the Cotton effect and this can be used for determination of enantiomeric excess. Notably, the CD magnitude of enantiopure carboxylates is enhanced by disparately sized substituents at the carboxylate stereocenter. The authors found that large differences in Taft substituent constants, E_s, of the medium and small substituents at the point stereocenter were positively correlated with the maximum CD signal observed. As we will see in later examples, this steric dependence is the basis of very useful linear free energy relationship considerations.

Figure 14. Suite of metal coordination complexes used for chirality sensing of carboxylates (39), alcohols (40), and primary amines (41).

Complex **40** utilizes a similar tripodal ligand scaffold for the ee determination of chiral alcohols via an iminium-bearing tripyridyl amine intermediate. Addition of a guest alcohol to the enantiotopic faces of the iminium produces a pair of diastereomers that can be quantified by NMR spectroscopy. 142,143 Similar to **39**, preferential formation of *M*- and *P*-helical stereoisomers produces Cotton effects around 260 nm with magnitudes that reflect the enantiopurity of the chiral alcohol with less than 3% error compared to chiral HPLC.

Ideally, complexes used for CD spectroscopy-based sensing produce far red-shifted signals. These regions are often devoid of CD signals originating from chiral ligands, which are common interferents present in asymmetric reactions. Di Bari and

Anslyn reported the octahedral Fe(II) complex 41 for ee determination of chiral amines that features an intense metal-toligand charge transfer (MLCT) band around 525 nm.144 The orientation of three ortho-iminopyridine ligands around a single metal center produces a statistical mixture of 24 stereoisomers. Although several of these species are present at once, the resultant CD spectrum still reflects the ee of the chiral amine because the complexes equilibrate according to the amine configuration and enantiopurity. Complex 41 is particularly well suited for high-throughput analysis because of its simple mix-andmeasure procedure, a common feature between complexes 39-41. A frequently encountered issue with chiroptical ee determination is the deconvolution of yield and enantiopurity. For instance, high concentration samples with low enantiopurity give similar CD intensities to low concentration samples and high enantiopurity. Sensor 41 was used in combination with a iminebased fluorescent indicator displacement assay to discern both yield and enantioenrichment, which enabled comprehensive reaction analysis.

The Zonta group developed the versatile vanadium sensor **42** which was successfully tested with an amine, amide, amino alcohol, α -hydroxy ester, cinchona alkaloid, sulfoxide, sulfoximine, *N*-oxide, phosphoric acid and a few carboxylic acids, Figure 15.⁵³

12 8 4 g-factor \times 10° -8 -12 λ (nm) q-factor × 10 4,0 3,0 2.0 1.0 ee (%) 100 -100 -50 50 -1.0 -2,0 -3.0 -4,0

Figure 15. Sensing with the vanadium complex **42** (top). Concentration-independent ee response between 590 and 620 nm of the vanadium complex **43** (bottom). Modified with permission from ref. [53]. Copyright 2017 American Chemical Society.

Coordination of an analyte to the metal center induces a remarkable color shift from orange to deep blue, which was attributed to the formation of the octahedral complex 43. This colorimetric change coincides with the induction of large CD signals at long wavelengths. The inspection of calibration curves developed with 42 and 44 at varying concentrations revealed a linear correlation between the anisotropic g-factor ($g = \Delta \epsilon/\epsilon$) obtained between 590 and 620 nm and the enantiomeric excess of the sample. With the g-factor in hand, the group was thus able to determine ee values independently from the analyte and sensor concentrations, a very useful facet that can be implemented into other assays where the chiroptical absorbance measured exclusively originates from the sensor-analyte adduct.

Chiroptical sensing based on metal coordination even enables ee and concentration determination of terpenes and terpenoids, such as 47-57, containing in some cases one or two double bonds as the only functional group. 63 The alkene binding occurs almost instantaneously under mild conditions when rhodium(I) chlorides 45 are treated with AgOTf or another silver salt to generate a free coordination site via irreversible halide abstraction which sets the stage for the formation of 46. Strong ICD effects at long wavelengths were observed with 18 alkenes tested using either pre-assembled or *in-situ* generated Rh(I) phosphine complexes, Figure 16. This chiral alkene sensing protocol was applied in the quantitative analysis of 12 α - and β -pinene samples and found to proceed with relatively small errors ranging from 0.3 to 4.6%.

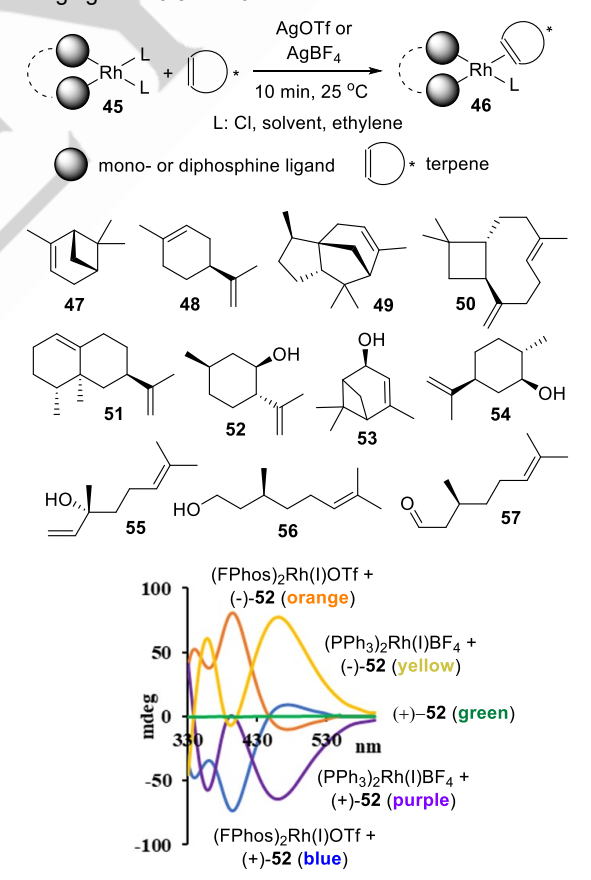


Figure 16. Rapid chiral alkene sensing with Rh(I) complexes generated *in-situ* with triphenylphosphine or tris(pentafluorophenyl)phosphine, FPhos. Modified with permission from ref. [63]. Copyright 2020 American Chemical Society.

3.3. Dynamic Covalent Chemistry

Sensing of amines, amino alcohols and amino acids based on the principles of dynamic covalent chemistry (DCC), in particular reversible Schiff base formation, has been among the most popular approaches. 73,74,145 The Baik, Yoon and Kim groups developed the amino alcohol sensor 58 which produces a BODIPY-like structure 60 displaying strong CD and fluorescence signals even when purely aliphatic substrates such as alaninol are incorporated, Figure 17.146 The boronic acid unit reacts with the alcohol moiety of the substrate forming a boronic ester intermediate followed by rapid formation of an intramolecular ketimine bond. DFT studies showed that the binding of the hydroxyl group facilitates the condensation reaction which occurs smoothly under mild conditions. CD signals at 425 nm and above were observed with a series of six chiral amino alcohols. The striking chiroptical responses generated by 58 are advantageous for concentration and ee analysis.

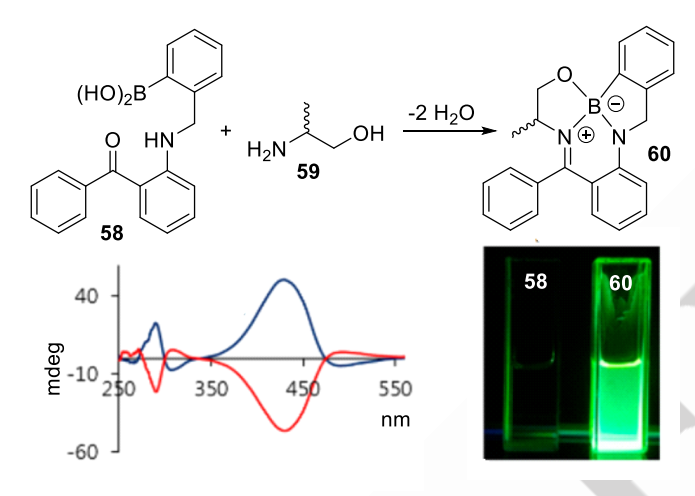


Figure 17. Sensing of amino alcohols by *in situ* formation of a BODIPY-like chromophore. Modified with permission from ref. [69]. Copyright 2020 American Chemical Society.

Chin, Hong, Kim, and coworkers introduced the achiral 2,2'dihydroxybenzophenone probe 61 equipped with chromophoric tolylazo extensions. It adopts a helical conformation stabilized by two internal hydrogen bonds upon Schiff base formation with a chiral amino acid, Figure 18.66 The condensation reaction was performed in aprotic solvents under ambient conditions generating the imine 62 which produces strong, red-shifted ECCD spectra. High amplitudes were observed with twelve standard amino acids tested and a linear relationship between the induced CD intensity and the enantiomeric excess was reported. The rigid imine scaffold together with the two hydrogen bond motifs produce a helical orientation in 62 that can be systematically correlated to the point chirality of the amino acid, i.e., (S)-valine favors population of the P form while (R)-valine will induce the M form. The consistent relationship between the sign of the observed Cotton effects and the chirality of the substrate opens the door to simultaneous analysis of sample ee and absolute configuration.

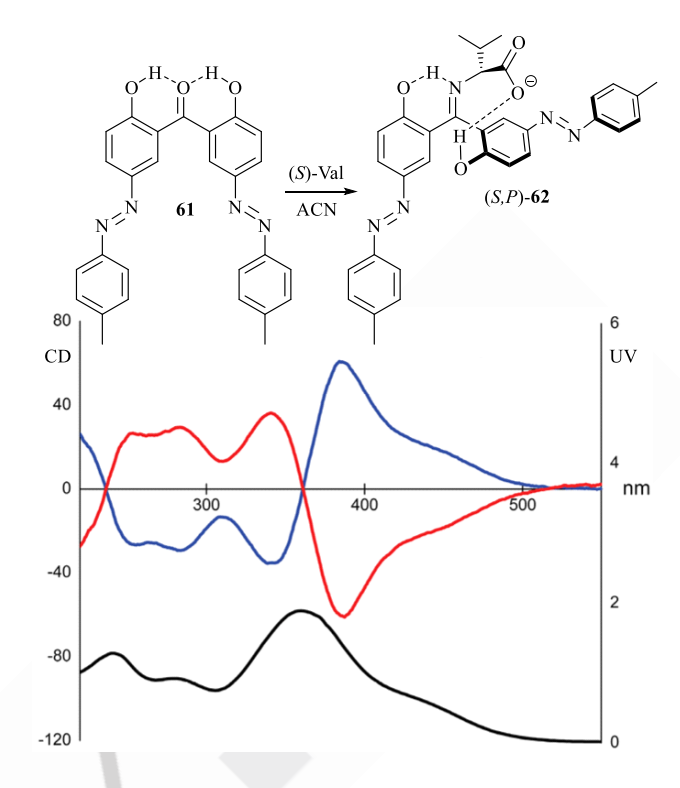


Figure 18. CD and UV spectra of the imines formed from the benzophenone derivative **61** and (*S*)-Val (blue) or (*R*)-Val (red). Modified with permission from ref. [66]. Copyright 2008 John Wiley & Sons.

You and Anslyn introduced biphenyl probe **63** for ee determination of several types of compounds, Figure 19.¹⁴⁷ The dynamic reaction between the sulfonamide and aldehyde groups provides a versatile scaffold with which alcohols, primary amines, and secondary amines can react to form CD-active diastereomers. For chiral alcohols, point-to-axial chirality transfer is achieved by nucleophilic addition to a cyclic iminium formed *in situ* from the aldehyde-sulfonamide pair, thus giving **64**. Primary and secondary amines react with the open and closed probe structure, respectively, toward **65** and **66**. In analogy to the biphenyl-derived probe introduced by Rosini shown in Figure 2,¹⁹ the proximity of the chiral guest introduces a preferential twist in the biphenyl core to produce the bisignate CD curve. This ability to accommodate a variety of chiral analytes is a distinct advantage of many DCC-based chiroptical sensors.

Figure 19. Interconverting biphenyl scaffold of **63** and reversible covalent binding of chiral mononucleophiles.

3.4. Supramolecular Systems

Macrocycles and foldamers have received increasing attention in recent years. 148-157 Key advantages of chiroptical sensing with inclusion complexes are fast exchange kinetics, high association constants when aqueous solvents are used to facilitate guest binding into the hydrophobic interior, and independence from binding motifs that would necessitate a suitable functional group in the analyte. Compared to other CD sensing strategies, relatively weak CD effects appearing at short wavelengths are typically produced and competitive binding equilibria with other small molecules present in more complicated mixtures may cause unpredictable interferences. Notwithstanding these issues, supramolecular systems hold considerable promise and future developments are likely to conquer new chiroptical sensing applications.

In their seminal work, Biedermann and Nau used cucurbit[8]uril, **67**, a rigid container with a hydrophobic cavity that has sufficient space for hosting two small molecules, to engage a dye like **68** or **69** and a chiral analyte in close contact interactions, Figure 20.⁴⁴ The only role of the UV-transparent cucurbituril is to pair the guests in a restricted environment thus enforcing π -stacking conducive to CD signal induction. Ternary complexes displaying distinct chiroptical properties were obtained with a variety of aromatic analytes including amino acids, peptides, drug molecules and natural products. Real-time monitoring of a kinetic resolution and of racemization reactions was also demonstrated.

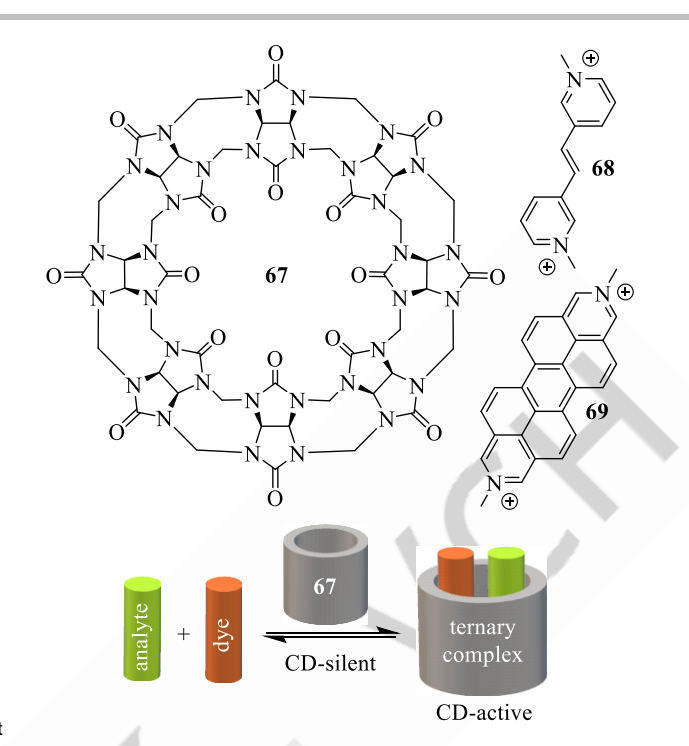


Figure 20. Formation of ternary inclusion complexes.

The use of conformationally flexible, chromophoric hosts can eliminate the need for a dye additive and achieve ee sensing through formation of a binary inclusion complex. Nau and Isaacs independently showed that acyclic cucurbituril-type receptors with aromatic extensions, such as 70 and 71, are inherently chiral and adapt rapidly interconverting helical structures that can accommodate a large variety of compounds, Figure 21.45,158 The interactions with a chiral guest molecule disturbs the equimolar equilibrium between the enantiomeric conformations of 70 or 71 and thus forms unequally populated CD-active diastereomers which allows ee determination of amines, alcohols, amino acids, peptides, terpenes, and steroids with a simple mixand-measure protocol. The complexation and imprinting of the guest chirality onto the stereodynamic receptor are fast processes and CD measurements can be performed without delay at micromolar concentrations.

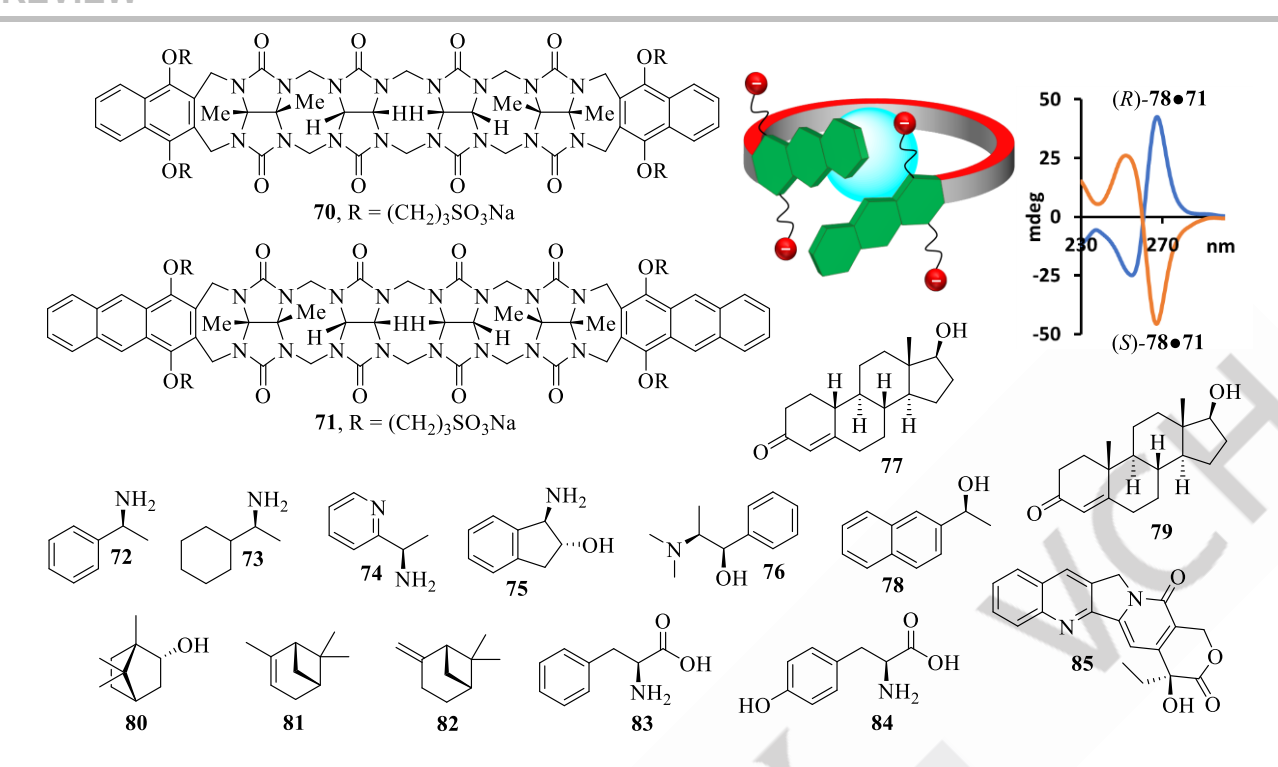


Figure 21. ICD sensing with helical cucurbituril-like hosts and representative analytes. Adapted with permission from ref. [158]. Copyright 2021 RSC Publishing.

The Jiang group has introduced achiral naphthotubes like **86** and showed impressive CD sensing applications, Figure 22.⁴⁶⁻⁴⁹ This type of chromophoric host binds a variety of organic molecules, including challenging aliphatic epoxides, alcohols, and many others, with high affinity in aqueous solvents. The inclusion complex formation induces a chiral conformation in the stereodynamic host, and this affords quantifiable CD signals. Both operational simplicity and speed are impressive. The analyte and sensor just need to be mixed, and the complexation, chirality imprinting, and CD induction are completed instantaneously, which creates new opportunities such as real-time monitoring of asymmetric reactions or other processes.

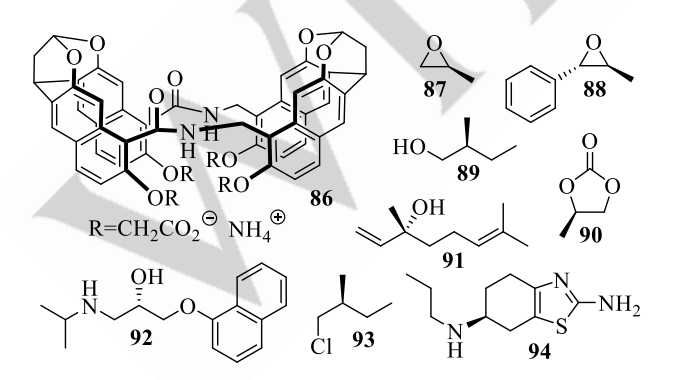


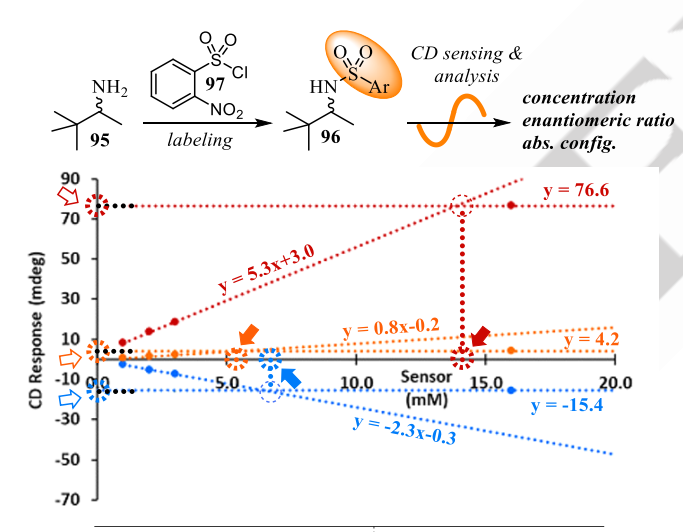
Figure 22. Structure of a stereodynamic naphthotube and selected target molecules.

4. Automation, High-throughput and Unified CD Sensing

As mentioned above, the compatibility of chiroptical sensing with automated equipment sets the stage for high-throughput experimentation and parallel sample analysis. Most assays require simple steps, i.e. dispensing of accurate amounts of solutions, mixing and dilution prior to the optical measurements. Today, the use of robotic pipetting instrumentation has become standard in many laboratories and 96 or 384-well microplate CD readers are commercially available to execute the whole operation automatically and with high precision. The Anslyn and Kahr laboratories pioneered the development of CD plate readers that can accommodate 96- and 384-well plates. 159,160 Typical CD spectrophotometers utilize cuvettes to hold single samples for analysis. While single acquisitions are quick, chiroptical ee determination requires calibration curves to be generated that may involve up to 10 separate acquisitions with enantioenriched standards. This experimental burden is magnified if different chiral compounds need to be analyzed, a general impediment that is essentially observed with any technique as each chiral analyte typically requires its own method development. However, CD microplate readers reduce this workload by allowing calibrations and experimental samples to be processed at once on the same plate. Once suitable calibration curves are obtained, parallel ee determination can be achieved with 4.5 s of measurement time per sample.

While most assays rely on a combination of CD spectroscopy with either UV or fluorescence measurements, it is also possible to determine both total analyte concentration and enantiomeric composition solely by CD analysis. 161 This was demonstrated with an achiral sulfonyl chloride probe **97** that reacts rapidly at room temperature with amines, amino alcohols

and amino acids, and affords a CD signal at 324 nm increasing linearly with the concentration and enantiopurity of the analyte, Figure 23. The basics of this "CD-only approach" is described using the sensing of nonracemic mixtures of 3,3-dimethylbutan-2amine, 95, present at varying amounts as an example. Sample 2 contains 95 in an enantiomeric ratio of 68.5:31.5 and a concentration of 7.0 mM (blue lines). A preliminary measurement revealed that the sulfonamide 96 obtained from probe 97 and enantiopure (S)-95 has a CD with a maximum of -84.0 mdeg at 14.0 mM. This value serves as reference in lieu of a calibration curve for the analysis of all 10 samples. When sample 2 was treated with excess of the probe, a CD intensity of -15.4 mdeg was measured. As long as 97 is applied in excess the same maximum CD value will always be measured, i.e., the strongest CD signal obtainable with sample 2 is -15.4 mdeg. This relationship is indicated by the horizontal blue line (y = -15.4)parallel to the x-axis. Note that the negative sign is used to assign the absolute configuration of the major enantiomer as S by comparison with the reference. When small quantities of probe 97 (1.0, 2.0, and 3.0 mM) were added to sample 2 only the corresponding fractions of the analyte present were consumed yielding steadily increasing CD responses at 324 nm. Plotting of these CD values against the concentration of probe 97 results in a slope indicative of the sample er (blue line, y = -2.3x-0.3). The sample concentration can now be determined as 6.5 mM from the projection of the intersection of the two blue dotted lines to the xaxis (see solid blue arrow).



	Samp	le coi	nposition	CD sensing results			
Entry	Conc. (mM)	AC	er	Conc. (mM)	AC	er	
1	5.0	S	55.0:45.0	4.0	S	55.5:45.5	
2	7.0	S	68.5:31.5	6.5	S	69.2:30.9	
3	10.0	S	85.0:15.0	10.3	S	84.6:15.4	
4	13.0	S	52.5:47.5	12.7	S	52.4:47.6	
5	90.0	S	99.0:1.0	8.7	S	98.8:1.2	
6	6.0	R	54.0:46.0	5.3	R	54.2:45.8	
7	8.0	R	81.5:18.5	7.6	R	81.9:18.1	
8	12.0	R	92.0:8.0	12.2	R	92.1:7.9	
9	14.0	R	65.0:35.0	13.6	R	64.8:35.2	
10	14.0	R	96.0:4.0	13.9	S	95.8:4.2	

Figure 23. Determination of absolute configuration, concentration and enantiomeric ratio of **95** using Wolf's unified CD sensing methodology. Adapted with permission from ref. [161]. Copyright 2022 Elsevier.

The er is then calculated using the previously mentioned CD_{max} of -15.4 mdeg obtained when sample 2 was treated with excess of the probe and the CD amplitude that enantiopure **96** would have at the actual sample 2 concentration which is readily available from the preliminary measurement (**96** affords -84.0 mdeg at 14.0 mM) mentioned at the beginning of this discussion. This simple mathematical analysis accurately determined the er of sample 2 as 69.2:30.9. The robustness of this approach, which was successfully applied to chromatography-free asymmetric reaction analysis, is shown with ten samples of **95**, of which three are graphically analyzed (2, 6 and 10) in the plot in Figure 23.

5. Asymmetric Reaction Screening

Asymmetric reaction development typically involves screening of many catalysts, additives, solvents, and variation of temperature among other parameters to pinpoint a combination that gives the desired product in satisfactory yield and ee. As a result, synthetic chemists often need to run hundreds of small-scale reactions in parallel to quickly cover a good fraction of the chemical space of interest. Modern high-throughput experimentation (HTE) equipment makes this an easy task, but the bottleneck is the reaction analysis which generally entails tedious product steps and subsequent chromatographic purification determination by processing one reaction at a time. Anslyn, 162-166 Arai, 167,168 Biedermann, 44 Jiang, 46,47 Joyce, 169 Wolf 65,131,161,170-172 and others have demonstrated how chiroptical sensing can resolve this analytical holdup, often by directly applying crude asymmetric reaction mixtures into their assays. 173

In one of the early examples of asymmetric reaction analysis, applied Brønsted/Lewis acid 98 was the mediated chlorodiisopinocampheylborane reduction of phenylglyoxlic acid, 99, to mandelic acid, 100.174 This sensor was designed to place a chiral α - or β -hydroxy acid between its urea and boronic acid moieties to imprint chiral bias onto its elongated π-system, which results in strong, red-shifted CD inductions and characteristic UV changes

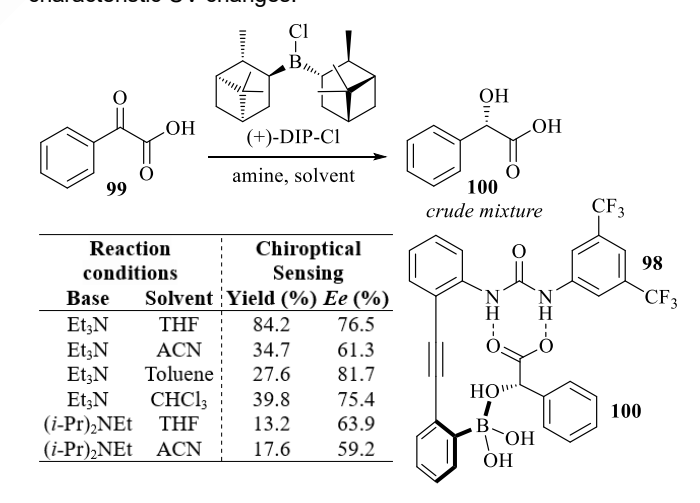


Figure 24. Asymmetric reaction screening with Wolf's Brønsted/Lewis acid 98.

The robustness of this bidentate molecular recognition motif enabled direct analysis of crude asymmetric reaction mixtures without traditional work-up, Figure 24. A total of 15 reactions with variations in solvent and amine additives were investigated with this sensor and results were compared to chiral HPLC runs of isolated 100. It was found that chiroptical sensing gives yields and ee's that deviate only by a few percent which is acceptable for high-throughput applications. Moreover, this assay is amenable to parallel analysis of hundreds of small-scale samples at increased speed and reduced waste generation, which are highly sought-after features that can greatly facilitate comprehensive asymmetric reaction optimization projects.

Another example of chiroptical analysis of reaction mixtures was presented by Miller and Anslyn, Figure 25.164 Aspartatebearing peptide catalysts were screened for activity in asymmetric Baeyer-Villiger oxidations using both chiral HPLC and alcohol sensor 40 to assess enantioselectivity. The chiral lactone product was hydrolyzed to afford a chiral alcohol, which could be analyzed with sensor 40. The chiroptical results compared well with HPLC runs (around 4% error) but requires only minimal preparation of the reaction mixtures as the residual ketone from incomplete oxidation does not interfere with the assay. The catalyst performance could be screened in just a few seconds compared to around 30 minutes per sample with HPLC. Along with ee determination, an additional benefit was the sensitivity of the sensor toward the structure of the alcohol. As previously discussed, the sign of the CD couplet is indicative of the absolute configuration of the analyte. Thus, the authors could rapidly identify the stereochemistry of the predominant enantiomer and the ee.

Figure 25. Sensing scheme for the ee determination of Baeyer-Villiger oxidation products with tripodal sensor 40.

6. Increasing the Sensing Space with Computation and Machine Learning

Given the recent uptick in using machine learning (ML) techniques in a variety of chemistry applications, it is no surprise to notice an already striking impact on the chiroptical sensing field. In fact, CD sensing is a well-known primary adopter of ML tools. Early examples include the use of chemometric approaches like linear discriminate analysis (LDA), a classification algorithm, to differentiate the CD response of a series of analytes. 141,175 Similarly, data-reduction algorithms like principal component analysis (PCA), a statistical technique used in many chemometric applications today, is frequently used to fingerprint chemical

identity and enantiopurity by training on CD spectra. Statistical techniques like PCA and LDA extend the use of linear free energy relationships (LFERs) to optimize sensor function and performance.43 For example, Anslyn and coworkers demonstrated that sterically bulky appendages (as measured by A-values and Taft parameters) on the tripodal ligand of 40 enhances the magnitude of the CD signal. This observation results from steric repulsion between the substituents of the incorporated analyte and the modified ligand. By tuning the steric interaction between incorporated analyte and the tripodal ligand, sensor 40 was reengineered to increase sensitivity towards βchiral alcohols. 176 Sensor optimization with LFERs compliment the rationally designed porphyrin tweezer systems for remote chirality sensing introduced by Borhan and coworkers. 1777,178

The use of LFERs in chiroptical sensing prompted further investigation into ML-guided probe design to target compounds with challenging remote stereocenters. Sigman and Anslyn exploited multiple linear regression (MLR) to elucidate physical organic properties that enable remote chirality sensing in 40.179 Taking inspiration from the data-driven optimization of asymmetric synthetic methods, density-functional theory chemical descriptors were used to characterize a diverse series of tripodal ligand derivatives with varying stereoelectronic properties, Figure 26. The selection of diverse ligands, a common practice in asymmetric catalysis, gave equally diverse outputs in sensitivity towards remote y-stereogenic alcohols. The authors identified a statistically robust MLR model that predicted the CD response of eight additional tripodal ligand derivatives. The model also uncovered valuable mechanistic insights by identifying proximal steric interactions to be important for maximizing the CD response when sensing γ-stereogenic alcohols.

$$Z_{n}$$
 A_{0}
 R_{2}
 A_{0}
 R_{2}
 R_{2}
 R_{3}
 R_{2}
 R_{3}
 R_{40}
 R_{2}
 R_{2}
 R_{3}
 R_{40}
 R_{2}
 R_{40}
 R_{2}
 R_{40}
 R_{2}
 R_{40}
 R_{2}
 R_{3}
 R_{40}
 R_{2}
 R_{40}
 R_{40}
 R_{2}
 R_{40}
 R_{4

Figure 26. Derivatized sensor 40 (top) and example aromatic substituents tested for MLR development (bottom).

The importance of these steric interactions, as measured by Sterimol parameters, 180 were confirmed by the presence of attractive non-covalent interactions (NCIs) involving the aryl group substituent on the tripodal ligand. Depending on the configuration of the γ -stereogenic alcohol, either the M- or P-axial stereoisomer of 40 is stabilized by attractive $\pi\text{-}\pi$ interactions and London dispersion forces. This stabilization magnifies the MIP diastereomeric ratio and enhances the CD intensity.

ML techniques can also be used to improve chirality sensing workflows and extend applications to unknown sample targets where references do not exist. Like any other analytical technique, quantitative chiroptical sensing requires calibration with enantioenriched standards that can be costly and time-consuming to prepare. Moreover, each analyte of interest must have its own calibration curve, which further slows chiroptical analysis if more than one analyte is targeted. By contrast, computational prediction of calibration curves removes the need for enantioenriched standards to calibrate chiroptical methods and can thus accelerate and extend asymmetric reaction development beyond currently perceived boundaries. 181 Towards this endeavor, Wolf and Anslyn applied MLR to the prediction of calibration curves for a stereodynamic bisnaphthol-based assay with the compound 105, Figure 27. Like the MLR techniques applied in the optimization of sensor 40, the magnitude of the CD signal of enantioenriched analytes can be predicted from physical organic descriptors obtained by density functional theory (DFT) calculations. A library of α-chiral primary amines was screened, and DFT calculations of the sensor assembly were performed to extract steric and electronic descriptors. Using the CD spectra and DFT descriptors as a training set, an MLR model was generated to predict calibration curves. The findings of this study agreed with previous reports of differential steric size of the stereocenter substituents to be a major component in inducing the resultant CD signal intensity. The predicted CD values were successfully used to generate theoretical calibration curves for the ee determination of chiral amines within 10% experimentally generated curves. 182

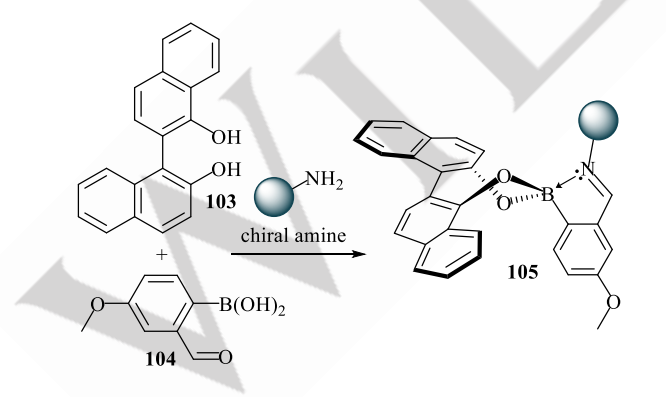


Figure 27. Three-component assembly for the \emph{ee} determination of chiral amines.

7. Chiral Compound Mixture Analysis

The ability of chiroptical sensing methods to process mixtures without sample purification can drastically streamline traditionally slow chiral compound screening workflows. Cysteine- and

homocysteine-specific receptors that allow determination of the concentration and enantiomeric composition in aqueous mixtures containing other amino acids, biothiols or peptides have been introduced. 183-185 While the total amount and ee of cysteine and homocysteine were successfully analyzed in complicated mixtures, the co-present amino acids were left unquantified. In some cases, comprehensive mixture analysis can be achieved because a probe generates strikingly different, non-overlapping CD signatures with different compounds, a rare scenario that has been exploited a few times. 186,187 The simultaneous ee sensing of mixtures of several analytes without physical separation is a highly sought-after goal in countless laboratories interested in fast chiral compound development. First examples showing that this is generally possible have appeared in the literature.

To date, few reports have addressed the common need to analyze mixtures that contain not only enantiomers but also diastereomers, mainly due to the difficulty with deconvoluting largely overlapping spectra. The Anslyn and Wolf groups showed independently that this is possible for vicinal amino alcohols by using reaction-based sensing methods in combination with supervised machine learning tools to solve the daunting analytical tasks. 188, 189 In Anslyn's protocol, protection of the amino group in 2-aminocyclohexanol **106** sets the stage for *er* analysis, Figure 28. The N-protected analyte 108 forms a Zn(II) assembly producing CD spectra that can be correlated to the stereochemistry at C-1. Schiff base formation of 106 with 111 and subsequent complexation to an iron(II) center, gives quantitative stereochemical information on C-2 via straightforward CD spectroscopic measurements, and UV-Vis analysis of the same assembly allows for the determination of the sample dr. The acetylated analyte 108 is then oxidized to the corresponding ketone 112 followed by hydrazone formation with 113 to afford 114 which is used for determination of the total concentration of 2-aminocyclohexanol by fluorescence spectroscopy.

The Wolf group developed a continuous workflow that does not require protection chemistry. Here, stereoisomeric mixtures of aminoindanol were analyzed solely by CD and UV-Vis spectroscopy. The total concentration and dr can be determined via UV-vis spectroscopy after Schiff base formation of 115 with salicylaldehyde, 116. Then, two sets of CD spectra are collected for er determination. The first set is obtained after addition of a Cu(II) salt to the solution of 117. Finally, one equivalent of tetrabutylammonium hydroxide is added to the same mixture to generate a second, substantially altered CD spectra set. The Anslyn group used 70 training samples to train a sequential and orthogonalized covariance selection (SO-CovSel) algorithm. A total of 10 samples with varying compositions were successfully analyzed with a maximum absolute error of 12.7%. The Wolf group used 20 training samples to train a linear programming algorithm and a parameter sweep algorithm for unbiased wavelength selection across the two data sets. The individual concentrations of each stereoisomer in 20 samples were determined with a maximum absolute error of 8.0%. Both reports are expected to be applicable to other amino alcohols and, more generally, demonstrate the prospect of chiroptical sensing methodology for separation-free analysis of mixtures of stereoisomers.

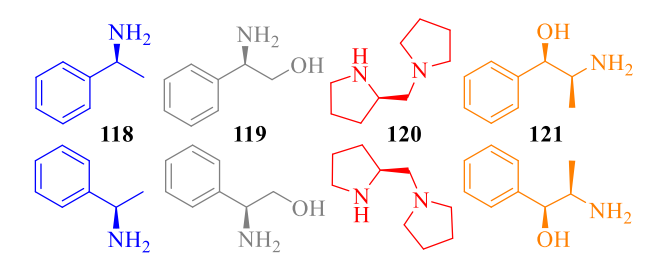
Figure 28. Anslyn's and Wolf's workflows for quantitative optical sensing of mixtures of four amino alcohol stereoisomers.

Deconvolution of complicated and largely overlapping spectra obtained with multicompound mixtures remains one of the major challenges in chiroptical sensing. 190-192 The Wolf group showed a solution to this problem by using the click chemistry probe 27, which features and applications are described in Section 3.1., and multiblock chemometric analysis to quantify each enantiomer of 118-121.193 To maximize the spectral information available for this daunting task, coumarin 27 was first applied to octonary samples containing various amounts and enantiomeric compositions of these amines and amino alcohols and the reaction mixtures were then diluted either with methanol or dichloroethane. Thus, four large data sets (two UV and two CD spectra) with increasingly distinguishable chiroptical spectra due to variance in intramolecular hydrogen bonding in these solvents were obtained. Following relatively short algorithm optimization with training samples, analysis with a multiblock partial least squares (MBPLS) method capable of orthogonal data fusion, i.e. incorporation of all four data sets, gave the analyte compositions with remarkable accuracy, Figure 29.

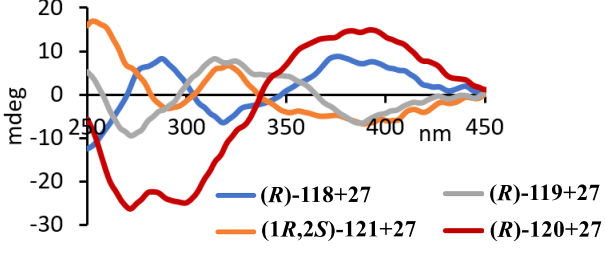
8. Timeline for Assay Creation

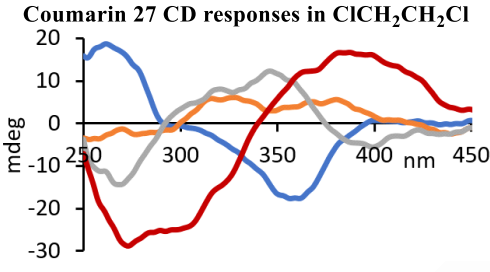
Chiral HPLC method development requires a racemic sample to be analyzed before screening real samples with potentially enantioenriched compounds. First, different chiral stationary phases (CSPs) and chromatographic conditions can be screened until adequate enantioresolution, that is, baseline separation of the enantiomers, is achieved. This is often a trial-and-error approach that can easily consume several hours or even days. Once chiral HPLC conditions are identified, the analysis of each

sample often requires 10 to 30 minutes depending on the separation conditions, as indicated by countless reports of asymmetric reaction developments. In some cases, chiral separations can be achieved within one minute, in particular when a supercritical fluid chromatography instrument is available. But this requires a previously isolated, chemically pure sample, i.e., crude mixtures containing interfering impurities that are likely to co-elute in such a short time frame cannot be analyzed directly with such a method. Since chromatographic methods are serial in nature, samples are examined one-by-one, and the analysis time of large sample numbers can add up substantially. While it is often necessary to run a mobile phase gradient and to recondition the column between each sample injection such additional analysis delay will not be considered here, but we note that this is not a problem with chiroptical assays. If a new compound is introduced, for example, when an asymmetric reaction with another substrate is screened, a racemic sample must be generated beforehand to develop a chiral HPLC method once again. Assuming similar conditions can be applied, the analysis of a new chiral compound requires two HPLC separations to determine ee. The testing and calibration of a chiroptical method requires two enantioenriched samples of different ee values to be measured, but typically 5 to 10 standards are used to generate calibration curves over a range of ee values. The identification and implementation of a suitable assay may take a few hours. Samples can then be analyzed in parallel. Some sensors require just 5 minutes of mixing time, but others necessitate a several hour equilibration period before the CD spectrum can be measured. With the advent of CD microplate readers, this can be inconsequential because large batches of samples in 96- and 384-well plates can be prepared and equilibrated in parallel, and then rapidly analyzed. If a new compound is introduced, an analyte-specific calibration curve must also be generated before analysis.



Coumarin 27 CD responses in MeOH 20 ¬





MBPLS/coumarin sensing results

Sample		(R)-	(S)-	(R)-	(S) -	(R)-	(S) -	(1S,2R)-	(1R,2S)-
		118	118	119	119	120	120	121	121
1	Act.	3.38	1.13	4.13	1.38	4.13	1.38	3.38	1.13
	Pred.	3.30	1.29	4.07	1.30	4.06	1.29	3.30	1.33
2	Act.	5.69	0.81	3.06	0.44	3.06	0.44	5.69	0.81
	Pred.	6.25	0.77	2.95	0.06	2.97	0.03	6.25	0.69
3	Act.	0.94	1.56	2.81	4.69	2.81	4.69	0.94	1.56
	Pred.	0.84	1.89	2.52	4.68	2.53	4.57	0.84	2.04
4	Act.	0.56	3.94	0.69	4.81	0.69	4.81	0.56	3.94
	Pred.	0.72	3.44	0.80	4.96	0.78	4.98	0.72	3.49
5	Act.	3.85	1.65	3.15	1.35	3.15	1.35	3.85	1.65
	Pred.	4.22	1.65	3.29	0.95	3.27	1.02	4.22	1.59
6	Act.	3.94	0.59	4.81	0.69	4.81	0.69	3.94	0.56
	Pred.	3.73	0.70	5.33	0.29	5.36	0.35	3.73	0.69

Figure 29. Chiroptical sensing of octonary analyte mixtures by MBPLS analysis. The different CD responses of **27** to the chiral analytes in methanol and dichloroethane are shown. All concentrations are in mM. Act. (Actual concentration). Pred. (Predicted concentration). Modified with permission from ref. [193] under terms of the CC-BY license.

Consider the analysis of two 96-well plates (192 samples) of reactions from an HTE optimization campaign of an asymmetric transformation, Figure 30. For chiral HPLC, we will assume that chromatographic conditions are identified in 2 hours and each sample requires 10 minutes to analyze. The whole batch would be processed in 34 hours wherein each sample is analyzed sequentially. Using a chiroptical method and assuming also a 2-hour period for the assay setup, each plate could be treated with the appropriate conditions at once and allowed to equilibrate for 5 hours — a typical equilibration period for metal complex-based

assays like sensor **15**, although other assays take just 5 minutes. If the CD spectra were acquired with a CD microplate spectrometer, the measurement time per sample is about 4.5 seconds resulting in ~15 minutes of total acquisition time. Thus, the entire procedure would require 7 hours and 15 minutes for all 192 reactions to be analyzed. However, if the mixing time is just 5 minutes, the total task would be completed in just 2 hours and 20 minutes. Altogether, chiroptical methods accelerate ee determination in projects where many enantioenriched samples of the same chiral compound need to be analyzed.

The application of ML techniques to chiroptical assays can further speed up ee determination by predicting calibration curves. As discussed above, ¹⁸² calibration curves can be predicted from MLR models created from chemical descriptors that are calculated with DFT methods. These models require numerous calculations that could take weeks to compute. However, once a suitable MLR model for a class of compounds is identified, a previously unknown analyte could be added by calculating only the specific parameters responsible for the difference in CD signal intensity. This eliminates preliminary testing and assay screening tasks and would avoid the need to create enantioenriched standards for calibration curves, thus dramatically reducing the experimental workload.

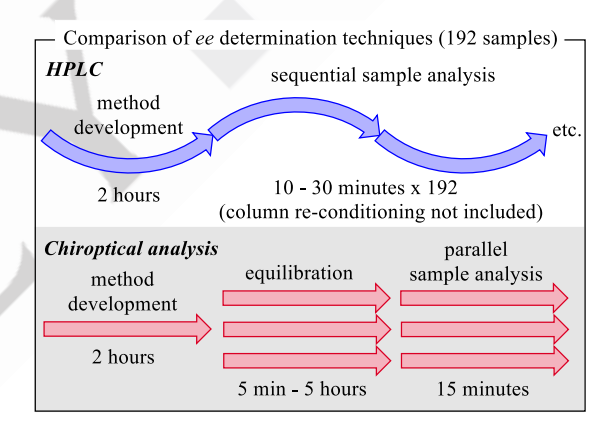


Figure 30. Comparison of the time required for ee determination with chiral HPLC and chiroptical methods.

9. Conclusions and Remarks

During the last few years, significant advances in the chiroptical sensing field, including vibrational CD, 194 fluorescence-detected CD8,195 and circularly polarized luminescence,196 have emerged. Increasingly rugged assays that are easy to adapt by any laboratory interested in high-speed analysis are now available and several groups have demonstrated the possibility of crude asymmetric reaction analysis. Among the most notable achievements are the introduction of sensors that can handle molecules exhibiting stereocenters far away from a functional group, real-time ee monitoring, for example of enzymatic reactions, the sensing of cryptochiral compounds, which are particularly difficult to analyze by chiral HPLC methods, the introduction of multi-variate analysis to predict calibration curves, and a few examples showing that the combination of chiroptical sensing and machine learning can be used for effective deconvolution of spectral overlap to realize chromatography-free multi-compound analysis. The significance of these and other

methodological developments is amplified by the introduction of commercially available automated CD plate readers, which sets the stage for high-throughput experimentation, for example, to speed up asymmetric reaction optimization tasks that are traditionally hampered by the dependence on arduous sample work-up protocols and chiral chromatography. To highlight this appealing prospect, we attempted above to compare the time required to measure ee using both chiral HPLC and chiroptical methods keeping in mind how most laboratories conduct such a task.

We anticipate that the CD assays discussed herein, and variations thereof, will play an increasingly important role in asymmetric synthesis developments and enable the discovery of new reactions at superior speed compared to currently used workflows and sequential sample handling practices. Chiroptical sensing, however, has applications beyond asymmetric reaction screening and is likely to find important biological and medicinal use. In fact, many assays applicable to aqueous solutions have been reported and found to allow accurate determination of the concentration and enantiomeric composition of free amino acids or other biomolecules. Despite impressive progress on various frontiers, several challenges remain. We notice that the field has made remarkable progress with optical enantiorecognition of amines, amino alcohols, amino acids and hydroxy acids while sensing of other compound classes remains underdeveloped and will likely require innovative, conceptually new solutions. Similarly, the chiroptical sensing space and applications need to be extended and this endeavor will undoubtedly benefit from the assistance of machine learning and chemometric data handling protocols that are already commonly used in combination with UV or other spectroscopic techniques. We hope that the readers of this Review will consider using chiroptical sensing in their daily routine and be inspired to pursue some of the remaining challenges in optical chiral compound analysis.

Acknowledgements

EVA gratefully acknowledges funding from the Welch Regents Chair (F-0046). CW gratefully acknowledges financial support from the NSF (CHE-2246747).

Conflict of Interest

The authors declare no competing financial interest.

10. References

- [1] C. L. Barhate, L. A. Joyce, A. A. Makarov, K. Zawatzky, F. Bernardoni, W. A. Schafer, D. W. Armstrong, C. J. Welch, E. L. Regalado, *Chem. Commun.* 2017, 53, 509–512.
- [2] S. Piovesana, R. Samperi, A. Laganà, M. Bella, Chem. Eur. J. 2013, 19, 11478–11494.
- [3] D. Leung, S. O. Kang, E. V. Anslyn, *Chem. Soc. Rev.* **2012**, *41*, 448–479.
- [4] L. Pu, Chem. Rev. 2004, 104, 1687-1716.
- [5] R. E Sonstrom, J. L. Neill, A. V. Mikhonin, R. Doetzer, B. H. Pate, *Chirality* 2022, 34, 114-125.
- [6] P. Tielmann, M. Boese, M. Luft, M. T. Reetz, Chem. Eur. J. 2003, 9, 3882-3887.
- [7] C. Wolf, K. W. Bentley, Chem. Soc. Rev. 2013, 42, 5408-5424.

- [8] A. Prabodh, Y. Wang, S. Sinn, P. Albertini, C. Spies, E. Spuling, L.-P. Yang, W. Jiang, S. Brase, F. Biedermann, Chem. Sci. 2021, 12, 9420-9431.
- [9] L. Yang, T. Wenzel, R. T. Williamson, M. Christensen, W. Schafer, C. J. Welch, ACS Cent. Sci. 2016, 2, 332-340.
- [10] S. M. Ramos De Dios, V. K. Tiwari, C. D. McCune, R. A. Dhokale, D. B. Berkowitz, Chem. Rev. 2022, 122, 13800–13880.
- [11] B. T. Herrera, S. L. Pilicer, E. V. Anslyn, L. A. Joyce, C. Wolf, J. Am. Chem. Soc. 2018, 140, 10385-10401.
- [12] S. Matile, N. Berova, K. Nakanishi, S. Novkova, I. Philpova, B. Blagoev, J. Am. Chem. Soc. 1995, 115, 7021-7022.
- [13] J. W. Canary, C. S. Allen, J. M. Castagnetto, Y. Wang, J. Am. Chem. Soc. 1995, 115, 8484-8485.
- [14] S. Superchi, D. Casarini, A. Laurita, A. Bavoso, C. Rosini, Angew. Chem., Int. Ed. 2001, 40, 451-454.
- [15] X. Huang, N. Fujioka, G. Pescitelli, F. E. Koehn, R. T. Williamson, K. Nakanishi, N. Berova, J. Am. Chem. Soc. 2002, 124, 10320-10335.
- [16] J. Zhang, A. E. Holmes, A. Sharma, N. R. Brooks, R. S. Rarig, J. Zubieta, J. W. Canary, *Chirality* 2003, 15, 180-189.
- [17] J.-P. Mazaleyrat, K. Wright, A. Gaucher, N. Toulemonde, M. Wakselman, S. Oancea, C. Peggion, F. Formaggio, V. Setnicka, T. A. Keiderling, C. Toniolo, J. Am. Chem. Soc. 2004, 126, 12874-12879.
- [18] J.-P. Mazaleyrat, K. Wright, A. Gaucher, N. Toulemonde, L. Dutot, M. Wakselman, Q. B. Broxterman, B. Kaptein, S. Oancea, C. Peggion, M. Crisma, F. Formaggio, C. Toniolo, *Chem. Eur. J.* 2005, 11, 6921-6929.
- [19] S. Superchi, R. Bisaccia, D. Casarini, A. Laurita, C. Rosini, J. Am. Chem. Soc. 2006, 128, 6893-6902.
- [20] A. E. Holmes, D. Das, J. W. Canary, J. Am. Chem. Soc. 2007, 129, 1506-1507
- [21] X. Li, M. Tanasova, C. Vasileiou, B. Borhan, J. Am. Chem. Soc. 2008, 130, 1885-1893.
- [22] L. Dutot, K. Wright, A. Gaucher, M. Wakselman, J.-P. Mazaleyrat, M. De Zotti, C. Peggion, F. Formaggio, C. Toniolo, J. Am. Chem. Soc. 2008, 130, 5986-5992.
- [23] S. Tartaglia, F. Pace, P. Scafato, C. Rosini, Org. Lett. 2008, 10, 3421-3424.
- [24] X. Li, B. Borhan, J. Am. Chem. Soc. 2008, 130, 16126-16127.
- [25] N. Berova, G. Pescitelli, A. G. Petrovic, G. Proni, Chem. Comm. 2009, 5958-5980.
- [26] J. Ściebura, P. Skowronek, J. Gawroński, Angew. Chem. Int. Ed. 2009, 48, 7069-7072.
- [27] J. Ściebura, J. Gawroński, Chem. Eur. J. 2011, 17, 13138-13141.
- [28] M. J. Kim, Y. R. Choi, H.-G. Jeon, P. Kang, M.-G. Choi, K.-S. Jeong, Chem. Commun. 2013, 49, 11412-11414.
- [29] J. Zhang, H. Gholami, X. Ding, M. Chun, C. Vasileiou, T. Nehira, B. Borhan, Org. Lett. 2017, 19, 1362-1365.
- [30] S. L. Pilicer, M. Mancinelli, A. Mazzanti, C. Wolf, Org. Biomol. Chem. 2019, 17, 6699-6705.
- [31] T. Mądry, A. Czapik, M. Kwit, J. Org. Chem. 2020, 85, 10413-10431
- [32] N. Prusinowska, A. Czapik, M. Kwit, J. Org. Chem. 2021, 86, 6433-6448.
- [33] H. Gholami, D. Chakraborty, J. Zhang, B. Borhan, Acc. Chem. Res. 2021, 54, 654-667.
- [34] S. Nieto, J. M. Dragna, E. V. Anslyn, Chem. Eur. J. 2010, 16, 227-232.
- [35] L. You, J. S. Berman, E. V. Anslyn, *Nat. Chem.* **2011**, *3*, 943-948.
- [36] L. A. Joyce, M. S. Maynor, J. M. Dragna, G. M. da Cruz, V. M. Lynch, J. W. Canary, E. V. Anslyn, J. Am. Chem. Soc. 2011, 133, 13746-13752.
- [37] J. M. Dragna, G. Pescitelli, L. Tran, V. M. Lynch, E. V. Anslyn, J. Am. Chem. Soc. 2012, 134, 4398-4407.
- [38] L. You, G. Pescitelli, E. V. Anslyn, L. Di Bari, J. Am. Chem. Soc. 2012, 134, 7117-7125.
- [39] L You, J. S. Berman, A. Lucksanawichien, E. V. Anslyn, J. Am. Chem. Soc. 2012, 134, 7126-7134.
- [40] H. H. Jo, C.-Y. Lin, E. V. Anslyn, Acc. Chem. Res. 2014, 47, 2212-2221.
- [41] H. M. Seifert, Y.-B. Jiang, E. V. Anslyn, Chem. Commun. 2014, 50, 15330-15332
- [42] X.-X. Chen, Y.-B. Jiang, E. V. Anslyn, Chem. Commun. 2016, 52, 12669-12671.
- [43] C. Lin, M.W. Giuliano, B.D. Ellis, S.J. Miller, E.V. Anslyn, *Chem. Sci.* 2016, 7, 4085-4090.
- [44] F. Biedermann, W. M. Nau, Angew. Chem. Int. Ed. 2014, 53, 5694-5699.

- [45] A. Prabodh, D. Bauer, S.; Kubik, P. Rebmann, F. G. Klärner, T. Schrader, L. Delarue Bizzini, M. Mayor, F. Biedermann, Chem. Commun. 2020, 56, 4652-4655.
- [46] L. L. Wang, Z. Chen, W. E. Liu, H. Ke, S. H. Wang, W. Jiang, J. Am. Chem. Soc. 2017, 139, 8436-8439.
- [47] L. L. Wang, M. Quan, T. L. Yang, Z. Chen, W. Jiang, Angew. Chem. Int. Ed. 2020, 59, 23817–23824.
- [48] X. Huang, X. Wang, M. Quan, H. Yao, H. Ke, W. Jiang, Angew. Chem. Int. Ed. 2021, 60, 1929-1935.
- [49] Y.F. Wang, H. Yao, L.-P. Yang, M. Quan, W. Jiang, Angew. Chem. Int. Ed. 2022, 61, e202211853.
- [50] F. A. Scaramuzzo, G. Licini, C. Zonta, Chem. Eur. J. 2013, 19, 16809-16813
- [51] E. Badetti, K. Wurst, G. Licini, C. Zonta, Chem. Eur. J. 2016, 22, 6515-6518.
- [52] N. A. Carmo dos Santos, E. Badetti, G. Licini, S. Abbate, G. Longhi, C. A. Zonta, Chirality 2018, 30, 65-73.
- [53] P. Zardi, K. Wurst, G. Licini, C. Zonta, J. Am. Chem. Soc. 2017, 139, 15616-15619.
- [54] F. A. Scaramuzzo, E. Badetti, G. Licini, C. Zonta, Eur. J. Org. Chem. 2017, 1438-1442.
- [55] F. A. Scaramuzzo, E. Badetti, G. Licini, C. Zonta, *Chirality* 2019, 31, 375-383.
- [56] M. W. Ghosn, C. Wolf, J. Am. Chem. Soc. 2009, 131, 16360-16361.
- [57] D. P. Iwaniuk, C. Wolf, J. Am. Chem. Soc. 2011, 133, 2414-2417.
- [58] K. W. Bentley, C. Wolf, J. Am. Chem. Soc. 2013, 135, 12200-12203.
- [59] K. W. Bentley, Y. G. Nam, J. M. Murphy, C. Wolf, J. Am. Chem. Soc. 2013, 135, 18052-18055.
- [60] K. W. Bentley, C. Wolf, J. Org. Chem. 2014, 79, 6517-6531.
- [61] K. W. Bentley, L. A. Joyce, E. C. Sherer, H. Sheng, C. Wolf, C. J. Welch, J. Org. Chem. 2016, 81, 1185-1191.
- [62] Z. A. De los Santos, R. Ding, C. Wolf, Org. Biomol. Chem. 2016, 14, 1934-1939.
- [63] Z. A. De los Santos, C. Wolf, J. Am. Chem. Soc. 2020, 142, 4121-4125.
- [64] E. Nelson, J. S. S. K. Formen, C. Wolf, Chem. Sci. 2021, 12, 8784-8790.
- [65] Z. A. De los Santos, C. C. Lynch, C. Wolf, Chem. Eur. J. 2022, 28, e202202028.
- [66] H. Kim, S. M. So, C. P. Yen, E. Vinhato, A. J. Lough, J. I. Hong, H. J. Kim, J. Chin, Angew. Chem. Int. Ed. 2008, 47, 8657-8660.
- [67] S. Nieto, V. M. Lynch, E. V. Anslyn, H. Kim, J. Chin, Org. Lett. 2008, 10, 5167-5170.
- [68] S. M. So, H. Kim, L. Mui, J. Chin, Eur. J. Org. Chem. 2012, 229-241.
- [69] M. E. Shirbhate, S. Kwon, A. Song, S. Kim, D. Kim, H. Huang, Y. Kim, H. Lee, S.-J. Kim, M.-H. Baik, J. Yoon, K. M. Kim, J. Am. Chem. Soc. 2020, 142, 4975-4979.
- [70] S. J. Wezenberg, G. Salassa, E. C. Escudero-Adan, J. Benet-Buchholz, A. W. Kleij, Angew. Chem., Int. Ed. 2011, 50, 713-716.
- [71] X. He, Q. Zhang, X. Liu, L. Lin, X. Feng, Chem. Commun. 2011, 47, 11641-11643.
- [72] X. Wu, X.-X. Chen, B.-N. Song, Y.-J. Huang, Z. Li, Z. Chen, T. D. James, Y.-B. Jiang, Chem. Eur. J. 2014, 20, 11793-11799.
- [73] M. S. Seo, A. Lee, H. Kim, Org Lett. 2014, 16, 2950-2953.
- [74] L. Joyce, E. Sherer, C. Welch, Chem. Sci. 2014, 5, 2855-2861.
- [75] R. Peng, L. Lin, W. Cao, J. Guo, X. Liu, X. Feng, Tetrahedron Lett. 2015, 56, 3882-3885.
- [76] M.-S. Seo, D. Sun, H. Kim, J. Org. Chem. 2017, 82, 6586-6591.
- [77] N. Berova, L. Di Bari, G. Pescitelli, *Chem. Soc. Rev.* **2007**, *36*, 914-931.
- [78] G. Pescitelli, Chirality 2022, 34, 333-363.
- [79] R. Katoono, H. Kawai, K. Fujiwara, T. Suzuki, J. Am. Chem. Soc. 2009, 131, 16896-16904.
- [80] K. Hor, O. Gimple, P. Schreier, H.-U. Humpf, J. Org. Chem. 1998, 63, 322-325.
- [81] M. Hartl, H.-U. Humpf, Tetrahedron: Asymm. 2000, 11, 1741-1747.
- [82] J. Gawronski, F. Kazmierczak, K. Gawronska, U. Rychlewska, B. Norden, A. Holmen, J. Am. Chem. Soc., 1998, 120, 12083-12091.
- [83] P. Skowronek, J. Gawronski, *Tetrahedron: Asymm.* **1999**, *10*, 4585-4590.
- [84] J. Gawronski, M. Kwit, K. Gawronska, Org. Lett. 2002, 4, 4185-4188.
- [85] S. Hosoi, M. Kamiya, T. Ohta, Org. Lett. 2001, 3, 3659-3662
- [86] S. Hosoi, M. Kamiya, F. Kiuchi, T. Ohta, *Tetrahedron Lett.* 2001, 42, 6315-6317.

- [87] T. Fujiwara, Y. Taniguchi, Y. Katsumoto, T. Tanaka, M. Node, M. Ozeki, M. Yamashita, S. Hosoi, *Tetrahedron: Asymm.* 2012, 23, 981-991.
- [88] L. Dutot, K. Wright, M. Wakselman, J.-P. Mazaleyrat, C. Peggion, M. De Zotti, F. Formaggio, C. Toniolo, *Tetrahedron Lett.* 2008, 49, 3475-3479.
- [89] S. Tartaglia, D. Padula, P. Scafato, L. Chiummiento, C. Rosini, J. Org. Chem. 2008, 73, 4865-4873.
- [90] J. Sciebura, P. Skowronek, J. Gawronski, Angew. Chem. Int. Ed. 2009, 48, 7069-7072
- [91] J. Sciebura, J. Gawronski, Chem. Eur. J. 2011, 17, 13138-13141.
- [92] A. E. Holmes, S. Zahn, J. W. Canary, Chirality 2002, 14, 471-477.
- [93] S. Zahn, J. W. Canary, Science 2000, 288, 1404-1407.
- [94] S. Zahn, J. W. Canary, Org. Lett. 1999, 1, 861-864.
- [95] H. S. Barcena, A. E. Holmes, S. Zahn, J. W. Canary, Org. Lett. 2003, 5, 709-711.
- [96] J. Zhang, A. E. Holmes, A. Sharma, N. R. Brooks, R. S. Rarig, J. Zubieta, J. W. Canary, *Chirality* 2003, **15**, 180-189.
- [97] T. Mizutani, T. Ema, T. Yoshida, Y. Kuroda, H. Ogoshi, *Inorg. Chem.* 1993, 33, 2072-2077.
- [98] M. Takeuchi, H. Kijima, I. Hamachi, S. Shinkai, Bull. Chem. Soc. Jpn. 1997, 70, 699-705.
- [99] Y. Furusho, T. Kimura, Y. Mizuno, T. Aida, J. Am. Chem. Soc. 1997, 119, 5267-5268.
- [100] S. Matile, N. Berova, K. Nakanishi, S. Novkova, I. Philipova, B. Blagoev, J. Am. Chem. Soc. 1995, 117, 7021-7022.
- [101] M. Balaz, M. De Napoli, A. E. Holmes, A. Mammana, K. Nakanishi, N. Berova, R. A. Purrello, *Angew. Chem. Int. Ed.* 2005, 44, 4006-4009.
- [102] X. Huang, K. Nakanishi, N. Berova, Chirality 2000, 12, 237-255
- [103] X. Huang, B. Borhan, B. H. Rickman, K. Nakanishi, N. Berova, *Chem. Eur. J.* 2000, 6, 216-224.
- [104] T. Kurtan, N. Nesnas, Y. Q. Li, X. F. Huang, K. Nakanishi and N. Berova, J. Am. Chem. Soc. 2001, 123, 5962-5973.
- [105] T. Kurtan, N. Nesnas, F. Koehn, Y. Q. Li, K. Nakanishi, N. Berova, J. Am. Chem. Soc. 2001, 123, 5974-5982.
- [106] X. Huang, B. H. Rickman, B. Borhan, N. Berova, K. Nakanishi, J. Am. Chem. Soc. 1998, 120, 6185-6186.
- [107] G. Proni, G. Pescitelli, X. Huang, N. Q. Quaraishi, K. Nakanishi, N. Berova, Chem. Comm. 2002, 1590-1591.
- [108] Q. Yang, C. Olmsted, B. Borhan, Org. Lett. 2002, 4, 3423-3426.
- [109] G. Proni, G. Pescitelli, X. Huang, K. Nakanishi, N. Berova, J. Am. Chem. Soc. 2003, 125, 12914-12927.
- [110] M. Tanasova, Q. Yang, C. C. Olmsted, C. Vasileiou, X. Li, M. Anyika, B. Borhan, Eur. J. Org. Chem. 2009, 4242-4253.
- [111] V. V. Borovkov, J. M. Lintuluoto, Y. Inoue, J. Am. Chem. Soc. 2001, 123, 2979-2989.
- [112] V. V. Borovkov, G. A. Hembury, Y. Inoue, Acc. Chem. Res. 2004, 37, 449-459.
- [113] H. Yoon, C.-H. Lee, W.-D. Jang, Chem. Eur. J. 2012, 18, 12479-12486.
- [114] X. Li, B. Borhan, J. Am. Chem. Soc. 2008, 130, 16126-16127.
- [115] X. Li, C. E. Burrell, R. J. Staples, B. Borhan, J. Am. Chem. Soc. 2012, 134, 9026-9029.
- [116] A. Petrovic, G. Vantomme, Y. Negrón-Abril, E. Lubian, G. Saielli, I. Menegazzo, R. Cordero, G. Proni, K. Nakanishi, T. Carofiglio, N. Berova, Chirality 2011, 23, 808-819.
- [117] M. Tanasova, B. Borhan, Eur. J. Org. Chem. 2012, 3261-3269.
- [118] H. Gholami, D. Chakraborty, J. Zhang, B. Borhan, Acc. Chem. Res. 2021, 54, 654-667.
- [119] M. Anyika, H. Gholami, K. D. Ashtekar, R. Acho, B. Borhan, J. Am. Chem. Soc. 2014, 136, 550-553.
- [120] H. Gholami, J. Zhang, M. Anyika, B. Borhan, Org. Lett. 2017, 19, 1722-1725.
- [121] H. Gholami, M. Anyika, J. Zhang, C. Vasileiou, B. Borhan, Chem. Eur. J. 2016, 22, 9235–9239.
- [122] D. Chakraborty, H. Gholami, A. Sarkar, L. A. Joyce, J. E. Jackson, B. Borhan, Chem. Sci. 2021, 12, 1750-1755.
- [123] S. Nieto, J. M. Dragna, E. V. Anslyn, Chem. Eur. J. 2010, 16, 227-232.
- [124] F. Y. Thanzeel, K. Balaraman, C. Wolf, Angew. Chem. Int. Ed. 2020, 59, 21382-21386.

- [125] A. C. Sedgwick, J. T. Brewster II, T. Wu, X. Feng, S. D. Bull, X. Qian, J. L. Sessler, T. D. James, E. V. Anslyn, X. Sun, Chem. Soc. Rev. 2021, 50, 9-38
- [126] S. L. Pilicer, P. R. Bakhshi, K. W. Bentley, C. Wolf, J. Am. Chem. Soc. 2017, 139, 1758-1761.
- [127] D. P. Iwaniuk, C. Wolf, Chem. Commun. 2012, 48, 11226-11228.
- [128] S. L. Pilicer, C. Wolf, J. Org. Chem. 2020, 85, 11560-11565.
- [129] Z. A. De los Santos, G. Yusin, C. Wolf, Tetrahedron 2019, 75, 1504-1509.
- [130] K. Osawa, H. Tagaya, S. I. Kondo, J. Org. Chem. 2019, 84, 6623-6630.
- [131] F. Y. Thanzeel, K. Balaraman, C. Wolf, Nat. Comm. 2018, 9, 5323.
- [132] S. L. Pilicer, J. M. Dragna, A. Garland, C. J. Welch, E. V. Anslyn, C. Wolf, J. Org. Chem. 2020, 85, 10858-10864.
- [133] B. Li, J. Zhang, L. Li, G. Chen, Chem. Sci. 2021, 12, 2504-2508.
- [134] P. Zhang, C. Wolf, Chem. Commun. 2013, 49, 7010-7012.
- [135] K. W. Bentley, Z. A. De los Santos, C. Wolf, Chirality 2015, 27, 700-707.
- [136] K. W. Bentley, L. A. Joyce, E. C. Sherer, H. Sheng, C. Wolf, C. J. Welch, J. Org. Chem. 2016, 81, 1185-1191.
- [137] Z. A. De los Santos, L. A. Joyce, E. C. Sherer, C. J. Welch, C. Wolf, J. Org. Chem. 2019, 84, 4639-4645.
- [138] Z. A. De los Santos, C. C. Lynch, C. Wolf, Angew. Chem. Int. Ed. 2019, 58, 1198-1202.
- [139] C. C. Lynch, Z. A. De los Santos, C. Wolf, Chem. Commun. 2019, 55, 6297-6300.
- [140] L. A. Joyce, M. S. Maynor, J. M. Dragna, G. M. da Cruz, V. M. Lynch, J. W. Canary, E. V. Anslyn, J. Am. Chem. Soc. 2011, 133, 13746-13752.
- [141] L. A. Joyce, J. W. Canary, E. V. Anslyn, Chem. Eur. J. 2012, 18, 8064-8069
- [142] L. You, G. Pescitelli, E. V. Anslyn, L. Di Bari, J. Am. Chem. Soc., 2012, 134, 7117-7125.
- [143] L. You, J. S. Berman, A. Lucksanawichien, E. V. Anslyn, J. Am. Chem. Soc., 2012, 134, 7126-7134.
- [144] J. M. Dragna, G. Pescitelli, L. Tran, V. M. Lynch, E. V. Anslyn, L. Di Bari, J. Am. Chem. Soc., 2012, 134, 4398-4407.
- [145] D. S. Hassan, F. Y. Thanzeel, C. Wolf, *Chirality* **2020**, *32*, 457-463.
- [146] M. E. Shirbhate, S. Kwon, A. Song, S. Kim, D. Kim, H. Huang, Y. Kim, H. Lee, S.-J. Kim, M.-H. Baik, J. Yoon, K. M. Kim, J. Am. Chem. Soc. 2020, 142, 4975-4979.
- [147] C. Ni, D. Zha, H. Ye, Y. Hai, Y. Zhou, E. V. Anslyn, L. You, *Angew. Chem. Int. Ed.* 2018, *57*, 1300-1305.
- [148] X. Liang, W. Liang, P. Jin, H. Wang, W. Wu, C. Yang, Chemosensors 2021, 9, 279.
- [149] M. Quan, X.-Y. Pang, W. Jiang, Angew. Chem. Int. Ed. 2022, 61, e202201258
- [150] M. Inouye, M. Waki, H. Abe, J. Am. Chem. Soc. 2004, 126, 2022–2027.
- [151] D. P. Iwaniuk, C. Wolf, Org. Lett. 2011, 13, 2602-2605.
- [152] Ie, M.; Setsune, J.-I.; Eda, K.; Tsuda, Org. Chem. Front. 2015, 2, 29-33.
- [153] J. B. Xiong, H. T. Feng, J. P. Sun, W. Z. Xie, D. Yang, M. Liu, Y. S. Zheng, J. Am. Chem. Soc. 2016, 138, 11469–11472.
- [154] Y. Chen, L. Fu, B. Sun, C. Qian, R. Wang, J. Jiang, C. Lin, J. Ma, L.Wang, Org. Lett. 2020, 22, 2266–2270.
- [155] H. Zhu, Q. Li, Z. Gao, H. Wang, B. Shi, Y. Wu, L. Shangguan, X. Hong, F. Wang, F. Huang, *Angew. Chem. Int. Ed.* 2020, 59, 10868–10872.
- [156] J. Ji, Y. Li, C. Xiao, G. Cheng, K. Luo, Q. Gong, D. Zhou, J. J. Chruma, W. Wu, C. Yang, *Chem. Commun.* 2020, 56, 161–164.
- [157] Y. Chen, L. Fu, B. Sun, C. Qian, S. Pangannaya, H. Zhu, J. Ma, J. Jiang, Z. Ni, R. Wang, X. Lu, L. Wang, Chem. Eur. J. 2021, 27, 5890–5896.
- [158] D. S. Hassan, Z. A. De los Santos, K. G. Brady, S. Murkli, L. Isaacs, C. Wolf, Org. Biomol. Chem. 2021, 19, 4248-4253.
- [159] P. Metola, S. M. Nichols, B. Kahr, E. V. Anslyn, Chem. Sci. 2014, 5, 4278-4282.
- [160] S. L. Pilicer, J. M. Dragna, A. Garland, C. J. Welch, E. V. Anslyn, C. Wolf, J. Org. Chem. 2020, 85, 10858-10864.
- [161] A. Sripada, F. Y. Thanzeel. C. Wolf, Chem 2022, 8, 1734-1749.
- [162] S. Nieto, J. M. Dragna, E. V. Anslyn, Chem. Eur. J. 2010, 16, 227-232.
- [163] Q. Zhao, J. Wen, R. Tan, K. Huang, P. Metola, R. Wang, E. V. Anslyn, X. Zhang, Angew. Chem. Int. Ed. 2014, 53, 8467-8470.
- [164] M. W. Giuliano, C-Y. Lin, D. K. Romney, S. J. Miller, E. V. Anslyn, Adv. Synth. Catal. 2015, 357, 2301-2309.

- [165] H. H. Jo, X. Gao, L. You, E. V. Anslyn, M. J. Krische, Chem. Sci. 2015, 6, 6747-6753.
- [166] J. Lim, M. Guo, S. Choi, S. J. Miller, E. V. Anslyn, Chem. Sci. 2023, 14, 5992-5999.
- [167] T. Arai, M. Watanabe, A. Fujiwara, N. Yokoyama, A. Yanagisawa, *Angew. Chem., Int. Ed.* 2006, 45, 5978–5981.
- [168] T. Arai, N. Yokoyama, A. Yanagisawa, Chem. Eur. J. 2008, 14, 2052-2059.
- [169] L. Joyce, E. Sherer, C. Welch, Chem. Sci. 2014, 5, 2855-2861.
- [170] K. W. Bentley, P. Zhang, C. Wolf, Science Adv. 2016, 2, e1501162.
- [171] Z. A. De los Santos, C. Wolf, J. Am. Chem. Soc. **2016**, 138, 13517-13520.
- [172] F. Y. Thanzeel, K. Balaraman, C. Wolf, Chem. Eur. J. 2019, 25, 11020-11025.
- [173] D. S. Hassan, F. S. Kariapper, C. C. Lynch, C. Wolf, Synthesis 2022, 54, 2527-2538.
- [174] K. W. Bentley, D. Proano, C. Wolf, Nat. Commun. 2016, 7, 12539.
- [175] S. Nieto, V. M. Lynch, E. V. Anslyn, H. Kim, J. Chin, J. Am. Chem. Soc. 2008, 130, 9232-9233.
- [176] M. B. Minus, A. L. Featherston, S. Choi, S. C. King, S. J. Miller, E. V. Anslyn, Chem 2019, 5, 3196–3206.
- [177] X. Li, C. E. Burrell, R. J. Staples, B. Borhan, J. Am. Chem. Soc. 2012, 134, 9026-9029.
- [178] M. Tanasova, M. Anyika, B. Borhan, Angew. Chem., Int. Ed. 2015, 54, 4274-4278.
- [179] J. J. Dotson, E. V. Anslyn, M. S. Sigman, J. Am. Chem. Soc. 2021, 143, 19187-19198.
- [180]~A.~Verloop,~W.~Hoogenstraaten,~J.~Tipker,~Drug Design~1976,~7,~165-207.
- [181] C.-Y. Lin, S. Lim, E. V. Anslyn, *J. Am. Chem. Soc.* **2016**, *138*, 8045-8047.
- [182] J. R. Howard, A. Bhakare, Z. Akhtar, C. Wolf, E. V. Anslyn, J. Am. Chem. Soc. 2022, 144, 17269–17276.
- [183] F. Y. Thanzeel, C. Wolf, Angew. Chem. Int. Ed. 2017, 56, 7276-7281.
- [184] F. Y. Thanzeel, L. S. Zandi, C. Wolf, Org. Biomol. Chem. 2020, 18, 8629-8632.
- [185] F. S. Kariapper, F. Y. Thanzeel, L. S. Zandi, C. Wolf, Org. Biomol. Chem. 2022, 20, 3056-3060.
- [186] J. S. S. K. Formen, C. Wolf, Angew. Chem. Int. Ed. 2021, 60, 27031-27038.
 [187] F. Y. Thanzeel, A. Sripada, C. Wolf, J. Am. Chem. Soc. 2019, 141, 16382-16387.
- [188] B. T. Herrera, S. R. Moor, M. McVeigh, E. K. Roesner, F. Marini, E. V. Anslyn, J. Am. Chem. Soc. 2019, 141, 11151-11160.
- [189] Z. A. De los Santos, S. MacAvaney, K. Russell, C. Wolf, Angew. Chem. Int. Ed. 2020, 59, 2440-2448.
- [190] Y. Sasaki, S. Kojima, V. Hamedpour, R. Kubota, S.-y. Takizawa, I. Yoshikawa, H. Houjou, Y. Kubo, T. Minami, Chem. Sci. 2020, 11, 3790-3796.
- [191] S. R. Moor, J. R. Howard, B. T. Herrera, M. S. McVeigh, F. Marini, A. T. Keating-Clay, E. V. Anslyn, Org. Chem Front. 2023, 10, 1286-1392.
- [192] F. Begato, R. Penasa, G. Licini, C. Zonta, ACS Sensors 2022, 7, 1390-1394.
- [193] D. S. Hassan, C. Wolf, Nat. Comm. 2021, 12, 6451.
- [194] R. Berardozzi, E. Badetti, N. A. C. dos Santos, K. Wurst, G. Licini, G. Pescitelli, C. Zonta, L. Di Bari, Chem. Commun. 2016, 52, 8428-8431.
- [195] R. Penasa, F. Begato, G. Licini, K. Wurst, S. Abbate, G. Longhi, C. Zonta, Chem. Commun. 2023, 59, 6714-6717.
- [196] J. Li, H.-Y. Zhou, Y. Han, C.-F. Chen, Angew. Chem. Int. Ed. 2021, 60, 21927–21933.

